

Block2: a comprehensive open source framework to develop and apply state-of-the-art DMRG algorithms in electronic structure and beyond

Huachen Zhai,^{a)} Henrik R. Larsson,^{b)} Seunghoon Lee,^{c)} Zhi-Hao Cui,^{d)} Tianyu Zhu,^{e)} Chong Sun,^{f)} Linqing Peng, Ruojing Peng, Ke Liao,^{g)} Johannes Tölle, Junjie Yang, Shuoxue Li, and Garnet Kin-Lic Chan^{h)}
Division of Chemistry and Chemical Engineering, California Institute of Technology, Pasadena, CA 91125, USA

(Dated: 9 October 2023)

BLOCK2 is an open source framework to implement and perform density matrix renormalization group and matrix product state algorithms. Out-of-the-box it supports the eigenstate, time-dependent, response, and finite-temperature algorithms. In addition, it carries special optimizations for *ab initio* electronic structure Hamiltonians and implements many quantum chemistry extensions to the density matrix renormalization group, such as dynamical correlation theories. The code is designed with an emphasis on flexibility, extensibility, and efficiency, and to support integration with external numerical packages. Here we explain the design principles and currently supported features and present numerical examples in a range of applications.

I. INTRODUCTION

The density matrix renormalization group (DMRG) algorithm^{1–3} is now a widely used numerical approach to obtain the low-energy eigenstates and other properties of a wide range of systems of interest in electronic structure, such as strongly correlated low-dimensional models,^{4–8} large active space problems in quantum chemistry,^{9–18} electronic quantum dynamics,^{19,20} and even models to benchmark quantum computing protocols.^{21,22} Over the last several decades, there have been many developments and extensions of the original algorithm for these applications.^{23–25} For example, dynamical electron correlation,^{26,27} the effects of finite temperature,^{28,29} relativistic effects,³⁰ time-dependent phenomena,³¹ and frequency-dependent³² response properties, can now all be treated within the DMRG framework.

In parallel with these theoretical advances, we have also witnessed the success of many different DMRG implementations for electronic structure,^{11,13,33–44} which together have helped demonstrate the power of DMRG in different settings. However, as more extensions of the DMRG algorithm have appeared and as DMRG techniques have grown to encompass more applications, so has the complexity grown in many implementations.

The new open source BLOCK2 code⁴⁵ introduced here, represents an effort to provide users with a comprehensive set of state-of-the-art DMRG algorithms used today in electronic structure and other applications, while enabling access to the development and extensions of these methods. To this end, the core design principles in BLOCK2 aim to balance efficiency, flexibility, and simplicity. For example:

(i) For efficiency and flexibility, we provide a special highly optimized DMRG implementation for the standard quantum chemistry Hamiltonian, but many of the optimizations also accelerate computations with arbitrary sparse Hamiltonians, thus enabling production level applications involving custom Hamiltonians.

(ii) For efficiency and simplicity, we provide both optimized and unoptimized implementations of most features in the code, so a developer can always start with the simplest version to explore new ideas, or compare different implementations to understand our optimization techniques. The framework supports both the matrix product state (MPS)/matrix product operator (MPO) and renormalized operator views of DMRG algorithms, balancing the ease of expressing algorithms with optimized performance.

(iii) For flexibility and simplicity, while the algorithms in BLOCK2 support general Hamiltonian and operator expressions, e.g. arbitrary-order interactions, arbitrary-order density matrix computations, and arbitrary-order excitations, the computations can be specified through a simple symbolic Python syntax.

We note that to achieve the above design goals, many implementations in BLOCK2 use techniques that to our knowledge have not been published in the literature. The following does not attempt to provide a full description of the implementation, which after all comprises approximately 200,000 lines of code. Instead, we introduce a sample of the existing features of BLOCK2, some ideas behind the implementation, and how the capabilities are used in applications and algorithm development.

^{a)}Electronic mail: hczhai.ok@gmail.com

^{b)}Present address: Department of Chemistry and Biochemistry, University of California, Merced, CA 95343, USA

^{c)}Present address: Department of Chemistry, Seoul National University, Seoul 151-747, Korea

^{d)}Present address: Department of Chemistry, Columbia University, New York, NY 10027, USA

^{e)}Present address: Department of Chemistry, Yale University, New Haven, CT 06520, USA

^{f)}Present address: Department of Chemistry, Rice University, Houston, Texas 77005, USA

^{g)}Present address: Department of Physics and Arnold Sommerfeld Center for Theoretical Physics, Ludwig-Maximilians-Universität München, D-80333 Munich, Germany

^{h)}Electronic mail: gkc1000@gmail.com

II. PROGRAM FEATURES

A. Standard DMRG

BLOCK2 provides a highly optimized and flexible implementation of the DMRG algorithm for solving various aspects of the electronic structure problem using *ab initio* and model Hamiltonians. This section presents an overview of the most common features of the code used in electronic structure calculations.

1. Ab initio DMRG and symmetries

The most common application of the *ab initio* DMRG algorithm is to compute a many-body ground state wavefunction with some desired symmetries.^{2,35,41,42,46–48} One first requires the Hamiltonian expressed in a basis of orthogonal orbitals, which form the sites in DMRG. Such orbitals, and the corresponding Hamiltonian integrals, can be computed by many quantum chemistry packages, for example, PySCF.^{49,50}

The Hamiltonian expressed in the chosen orbital basis typically has a number of symmetries. BLOCK2 has built-in efficient support for many different symmetries [including particle-number $U(1)$,³⁴ total spin $SU(2)$,³⁵ projected spin $U(1)$,³⁴ K -point Z_n ,⁵¹ $SO(4)$ in the Hubbard model,^{52,53} and the Abelian point group (D_{2h} and its subgroups²⁴)] and is designed to be easily extensible to other symmetries.

Fig. 1 illustrates the computational scaling with bond dimension of the *ab initio* DMRG algorithm implemented in BLOCK2 using different spin symmetries.

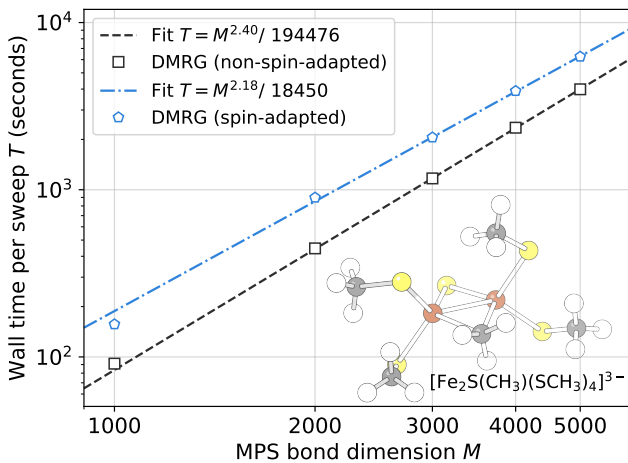


FIG. 1. The scaling of DMRG wall time (using 24 CPU cores) per sweep with respect to the MPS bond dimension M , for the (36o, 48e) active space of a protonated iron sulfur dimer $[\text{Fe}_2\text{S}(\text{CH}_3)(\text{SCH}_3)_4]^{3-}$. The active space model is from Ref. 54. Spin-adapted uses particle-number and $SU(2)$ symmetry, while non-spin-adapted uses particle-number and projected-spin $U(1)$ symmetry.

2. Sweep algorithms

Standard DMRG optimizations (sweeps) update the wavefunction in one of two ways, termed the two-site and one-site algorithms.^{2,55,56} The local Hilbert space in DMRG refers to the Fock space of the site, which is **of**, e.g. dimension $d = 4$ for a spatial orbital and $d = 2$ for a spin orbital. Assuming each DMRG site is a spatial orbital, the two-site algorithm uses the product space of the larger two-site local Hilbert space $d = 16$ and the left and right block renormalized states to represent the DMRG renormalized wavefunction (which helps escape from local minima) while the one-site algorithm substitutes the $d = 4$ local Hilbert space, lowering memory and computational costs. An effective “half-site” calculation with $d = 2$ can also be performed by using the one-site algorithm with spin orbital sites. One can also fuse sites in the sweep (by contracting adjacent tensors in the Hamiltonian matrix product operator (MPO)) before performing DMRG, allowing BLOCK2 to perform larger site sweep optimizations.

We note that the dimension of the local Hilbert space on different sites need not be the same. For example, DMRG algorithms with one or two large sites⁵⁷ use a single site to represent all the virtual and/or core orbitals to efficiently treat dynamic correlation. In such cases, BLOCK2 supports mixing the one-site and two-site sweep algorithms to balance efficiency and accuracy.⁵⁷

3. Excited states

The ground-state DMRG algorithm can be extended to optimize excited states and such excited-state algorithms are available in BLOCK2. The excited-state algorithms implemented in BLOCK2 take the following forms:

(i) The state-averaged DMRG approach.⁵⁸ In this formalism, there is a common set of rotation matrices for all states, but the center site carries a unique tensor (renormalized wavefunction) for each state. This algorithm is normally a robust and convenient choice for tens of roots, but for a given bond dimension, the accuracy decreases as the number of roots is increased.

(ii) The projected orthogonalization approach.^{40,59,60} To improve the quality of the states obtained from the state-averaged DMRG, one can further refine each excited state (as an independent MPS) by projecting out lower-lying states when optimizing the central site.

(iii) The level-shift approach.^{33,39} Here, we compute the ground and excited states one-by-one with a modified level-shifted Hamiltonian defined as

$$\hat{H}'_k = \hat{H} + \sum_{i=1}^{k-1} w_i |\Psi_i\rangle\langle\Psi_i| \quad (1)$$

where $|\Psi_i\rangle$ are the converged states below the targeted excited state $|\Psi_k\rangle$, and w_i are the energy level shifts.

This can be combined with the state-averaged ansatz to determine batches of states at a time.

(iv) The Harmonic Davidson approach.⁵⁸ By changing the standard Davidson solver to the Harmonic Davidson solver, one can directly target interior excited states close to a given energy without computing all the states below. In the current implementation of BLOCK2, this approach is not as stable as the above approaches for dense spectra.

4. Relativistic effects

Relativistic effects can be classified into scalar relativistic and spin-dependent relativistic effects,⁶¹ where the mean-field level scalar relativistic effects can be described inexpensively.⁶² BLOCK2 supports several strategies to include the scalar and spin-dependent relativistic effects.

(i) Relativistic DMRG.^{63–65} We can directly solve for eigenstates of four-component Dirac-Coulomb, Dirac-Coulomb-Gaunt, or Dirac-Coulomb-Breit Hamiltonians.⁶⁶ Here DMRG is performed in complex number mode where both the MPS and MPO are complex.

(ii) One-step SOC-DMRG.⁶⁷ Within the two-component formalism of relativistic quantum chemistry, we can include spin-orbit coupling (SOC) by adding a SOC term to the scalar-relativistic Hamiltonian, and then perform DMRG on this two-component Hamiltonian with a complex MPO and MPS. Alternatively, we can simplify the SOC term within the spin-orbit mean-field (SOMF) approximation,⁶⁸ giving rise to complex one-electron and real two-electron integrals. One can then represent the Hamiltonian as the sum of two MPOs where the expensive two-electron interaction is contained only in the second MPO, which is completely real.⁶⁷ One then runs BLOCK2 in the hybrid complex and real arithmetic DMRG mode, where the real and imaginary parts of the effective wavefunction share the same real rotation matrices in the MPS.

(iii) Two-step SOC-DMRG.^{30,69,70} When the SOC effect is weak, we can first compute eigenstates of the scalar-relativistic Hamiltonian. Then SOC effects can be added by carrying out the state-interaction of a small number of eigenstates.

Fig. 2 shows a numerical comparison of the accuracy of the 1-step and 2-step SOC-DMRG treatments.

5. Non-standard Hamiltonians and operators

In addition to computations involving the standard Hermitian quantum chemistry Hamiltonian with up to two-body interaction terms, BLOCK2 supports the use of other types of non-standard Hamiltonians and operators in DMRG algorithms and/or MPO/MPS operations.

(i) General Hamiltonians with high-order interactions. Using the techniques in Section II C, BLOCK2 supports

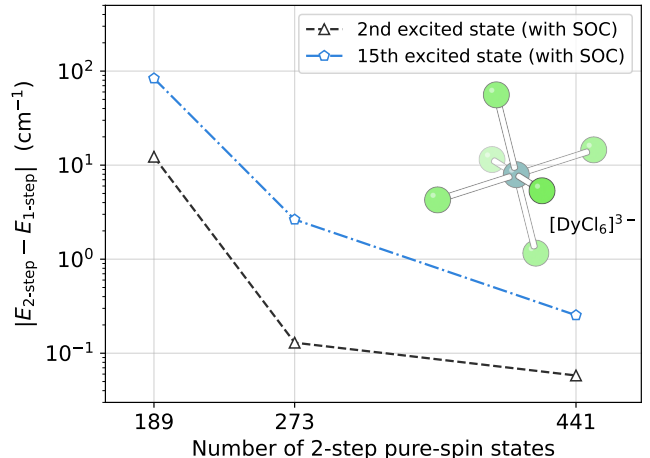


FIG. 2. The energy difference between representative excited states computed from the 1-step and 2-step SOC-DMRG approaches, for the (7o, 9e) active space of the $[\text{DyCl}_6]^{3-}$ cluster. Adapted from Fig. 4(a) in Ref. 67.

DMRG computations with arbitrary parity-preserving (i.e. even number of creation and annihilation operator) Hamiltonians. For example, DMRG calculations can be carried out for Hamiltonians with three-body or up to n -body terms. We note that higher than two-body terms appear commonly in quantum chemistry in effective Hamiltonians obtained from similarity transformations⁷¹ or canonical transformations^{72–75} of the *ab initio* Hamiltonians.

(ii) Normal-ordered Hamiltonians.⁷⁶ The DMRG algorithm can work instead with the normal-ordered version of a Hamiltonian where the vacuum expectation value is separated out. This can make the DMRG algorithm with reduced floating point precision numerically more stable.

(iii) Non-Hermitian Hamiltonians.^{71,77–79} This allows DMRG to be used, for example, with Hamiltonians that arise from many-body similarity transformations, such as in coupled cluster theory or the transcorrelated method.

(iv) Anti-Hermitian operators. BLOCK2 has special support for anti-Hermitian operators. Exponentials of anti-Hermitian operators appear in various applications, most notably, when performing orbital rotations of the MPS, or in canonical transformation theory.⁷³ The explicit support for anti-Hermitian operators allows such unitaries to be expressed as an exponential of a real MPO, thus avoiding complex arithmetic.

(v) General MPO and MPS operations with arbitrary operators. BLOCK2 supports MPO and MPS operations with arbitrary operators, including non-number-conserving operators, as described in Section II D. For example, to support the MPS compression approach for strongly-correlated NEVTP2,⁸⁰ one needs to apply a partial Hamiltonian to the reference wavefunction to get the

perturber wavefunction

$$|\Psi'_i\rangle = \sum_{abc} v_{iabc} a_a^\dagger a_b^\dagger a_c |\Psi_0\rangle \quad (2)$$

In BLOCK2 this is done by building an MPO for the operator part in the above expression.

6. Initial guesses

BLOCK2 provides several ways to generate initial MPS guesses for various algorithms. It also provides an implementation of perturbative noise^{55,56} which helps DMRG algorithms escape from poor initial guesses.

(i) A random MPS with the desired bond dimension can be generated.²⁴

(ii) One can supply an estimate of the occupancy information at each site from a cheaper method [e.g. coupled cluster singles and doubles (CCSD)]. BLOCK2 then uses this information to construct the initial quantum number distribution in the MPS.

(iii) We can generate an initial guess from another (more approximate) MPS using fitting. For example, we can use an MPS parameterized and optimized in the singles and doubles excitation space to initialize the MPS in the full Hilbert space.

7. Orbital reordering algorithms

For a given bond dimension, the accuracy of DMRG is affected by the orbital ordering.⁸¹ BLOCK2 provides several options to choose good orbital orderings in DMRG.

(i) For molecules with non-trivial point group symmetries, it can group the orbitals by irreducible representation.^{82,83}

(ii) For less symmetric systems, it can choose an ordering using the Fiedler vector⁸⁴ of an appropriate metric matrix. This ordering method is very inexpensive.⁸⁵

(iii) The Fiedler ordering can be further optimized using a more expensive genetic algorithm (GA),⁸⁵ as used in the STACKBLOCK code.⁵⁹ In BLOCK2, this GA is reimplemented with greatly increased efficiency.

The Fiedler and GA orderings require one to define a metric to measure the correlation between pairs of orbitals. BLOCK2 can use the absolute value of the exchange matrix⁸⁵ or the two-orbital mutual information [computed from the one- and two-orbital density matrices (1 and 2ODMs)]⁸⁶ for this purpose.

8. DMRG-CASSCF

For typical quantum chemistry problems, it is often not possible to treat all orbitals in DMRG. One can combine DMRG with the Complete Active Space Self-Consistent Field (CASSCF) method^{87,88} to use DMRG

to approximate the FCI problem within the active space while optimizing the active space orbitals.⁸⁹⁻⁹³ Using BLOCK2 we can perform DMRG-CASSCF through interfaces provided by external quantum chemistry packages, such as PySCF.^{49,50} With PySCF we currently support DMRG-CASSCF energy optimization⁹⁰ for spin restricted and spin unrestricted orbitals, and DMRG-CASSCF gradients and geometry optimization⁹² for spin restricted orbitals.

B. High performance DMRG

Parallelization in *ab initio* DMRG is essential to realistic chemical problems. In BLOCK2 we have implemented a hierarchy of different parallel and related DMRG strategies.

1. Standard parallelization strategies

In a recent report,⁹⁴ we summarized five standard parallel DMRG strategies implemented in BLOCK2: (i) parallelism over the sum of sub-Hamiltonians,⁹⁵ (ii) parallelism over sites,^{96,97} (iii) parallelism over normal and complementary operators,^{24,98} (iv) parallelism over symmetry sectors,^{11,99} and (v) parallelism within dense matrix multiplications.^{99,100} For large scale calculations, it is essential to combine these strategies to achieve high performance.⁹⁴

We have implemented most of these strategies in BLOCK2 not only for the ground state optimization problem, but also for other types of calculations, such as time evolution and the calculation of response properties. The user can change the parallelization strategy at runtime to maximize the efficiency of custom workflows.

Fig. 3 shows a numerical example of the performance of parallel DMRG.

2. Integral distribution strategies

In large *ab initio* calculations, the memory to store the two-electron integrals of the Hamiltonian can be a bottleneck. In BLOCK2 we provide several integral/MPO distribution strategies to balance the CPU, disk, and memory consumption in such calculations.

(i) In the default strategy for small- to medium-sized problems, integrals are replicated across different nodes, which provides the most flexibility for the DMRG algorithm. In this case, we have the freedom to switch between the normal/complementary (NC) parallelization strategy and the complementary/normal (CN) parallelization strategy near the middle site of a sweep,¹¹ which leads to higher computational efficiency.

(ii) For larger calculations where integral replication is problematic, we provide an alternative strategy where each node only stores the portion of integrals required

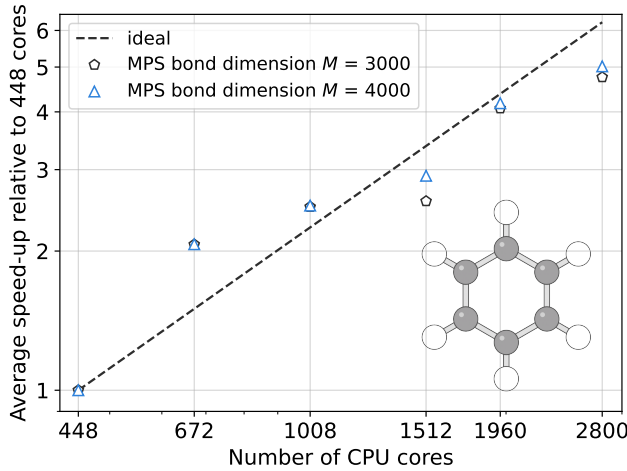


FIG. 3. Speed-up of average wall time per sweep relative to the $N_{\text{core}} = 448$ case for different MPS bond dimensions using parallel DMRG algorithms, for solving the ground state in a (108o, 30e) active space of the benzene molecule¹⁰¹ using a cc-pVDZ basis.¹⁰² Adapted from Fig. 4 in Ref. 94.

by that node. This strategy reduces the communication and memory costs, at the price of slightly reduced CPU efficiency.⁹⁴

(iii) When the number of orbitals is large and localization has been performed, there are many small or close-to-zero integral elements. BLOCK2 can store the integrals in a compressed format to further reduce memory consumption, using a floating point number compression algorithm introduced in Ref. 94. (Note that this only affects the memory consumption before the Hamiltonian MPO is built.)

(iv) For even larger scale applications, the MPOs constructed from the sub-Hamiltonians can also consume a large amount of memory on each node (since each MPO must contain at least the same amount of information as contained in the integrals). To alleviate this problem, we can store the MPO primarily on disk and only the MPO tensors required at the given one or two sites in an iteration of the sweep algorithm are loaded into memory. Note that MPO storage is not a problem in traditional DMRG implementations like STACKBLOCK where the action of the MPO is performed on the fly.

(v) At the cost of introducing some error, the bond dimension of the sub-Hamiltonian MPOs can be compressed during the construction as described in Section II C.

3. Parallelization strategies for specific tasks

The aforementioned parallelization strategies are common to a wide range of DMRG algorithms. We have additionally implemented more specialized parallelization strategies for some specific computational tasks.

(i) The generation of the Hamiltonian matrix elements in large-site DMRG calculations (used e.g. to treat multireference dynamical correlation⁵⁷) is implemented with shared-memory parallelization over the determinants or Configuration State Functions (CSFs).

(ii) Green's function calculations in dynamical DMRG¹⁰³ are parallelized in a distributed manner over the site index of the one-particle Green's function matrix element.

(iii) Stochastic perturbative DMRG¹⁰⁴ is implemented with a hybrid shared-memory and distributed parallelization to sample determinants or CSFs.

(iv) The GA algorithm for orbital reordering⁸⁵ is implemented with distributed parallelization over the different initial populations in a multi-start style GA algorithm.

(v) The MPS compression step in the DMRG version of second order strongly-contracted N -Electron Valence States for Multireference Perturbation Theory (SC-NEVPT2)⁸⁰ is implemented with distributed parallelization over virtual orbital indices.

C. General operators and MPO construction algorithms

BLOCK2 provides full support for algorithms involving general Hamiltonians (and other operators) expressed as MPOs. The implementation in BLOCK2 is carefully designed to support such general operations while not (severely) sacrificing efficiency. As discussed in Ref. 95, the original *ab initio* DMRG algorithm¹⁰⁵ implicitly provides an efficient implementation of the expectation value of a sparse MPO, but does not explicitly construct the MPO. The advantages of an explicit MPO object for relevant operators and Hamiltonians is that a wider variety of algorithms can be easily implemented. However, naive implementations of the MPO for complicated operators such as the *ab initio* Hamiltonian lead to the wrong cost scaling.⁹⁵ Consequently, BLOCK2 uses the techniques described below to achieve high efficiency.

1. Symbolic MPO approach for *ab initio* Hamiltonians

To obtain performance competitive with traditional implementations of *ab initio* DMRG (such as the one found in STACKBLOCK),^{34,35} BLOCK2 provides a symbolic MPO class for *ab initio* Hamiltonians. Here, the multiplication of the MPO matrices is interpreted as a set of formulae that reproduce the DMRG equations in traditional *ab initio* implementations. Symbolic MPOs are available for different spin symmetries: S^2 (SU2), S_z , and no spin symmetry, and support the Normal/Complementary (NC) partition, the Complementary/Normal (CN) partition, and the more efficient mixed partition with a NC to CN transformation near the middle site.¹¹ In addition, simplification rules are applied during the symbolic multiplication of the MPO matrices to use the in-

dex permutation and transposition symmetry of the normal and complementary operators¹¹ (such as $\hat{A}_{ij} = -\hat{A}_{ji}$ where \hat{A}_{ij} is defined as $a_i^\dagger a_j^\dagger$). This reduces the number of non-redundant renormalized operators that have to be stored and computed during DMRG sweeps. With this optimization, the DMRG algorithm implemented via the symbolic MPO is more memory efficient than with MPOs constructed using other approaches. In addition, because the symbols correspond to the labels of renormalized operators in a traditional DMRG algorithm, we can also implement conventional DMRG parallelization strategies in the literature within this MPO approach.^{95,98}

2. General MPO construction for Hamiltonians

BLOCK2 also implements general operator and Hamiltonian MPOs efficiently. At the interface level, the user writes the definition of the operator as a symbolic expression, using characters in a string to represent elementary operators such as \hat{a}^\dagger and \hat{a} . If non-standard elementary operators are required, the user can define the matrix representation of each elementary operator in a Python script. Bosonic operators^{106,107} and general Pauli strings⁸³ are supported. Starting from such an arbitrary symbolic expression of a many-body operator (such as the Hamiltonian), and the matrix representation of the involved elementary operators (in any local orthonormal basis), the code generates the MPO automatically. One can then use the MPO to optimize or evaluate expectation values, and carry out other DMRG computations. Both spin-adapted and non-spin-adapted MPOs can be generated. Listing 1 is an example Python script for performing DMRG of the Hubbard-Holstein model using BLOCK2.

```
from pyblock2.driver.core import DMRGDriver, SymmetryTypes, MPOAlgorithmTypes
import numpy as np

N_SITES_ELEC, N_SITES_PH, N_ELEC = 4, 4, 4
N_PH, U, OMEGA, G = 11, 2, 0.25, 0.5
L = N_SITES_ELEC + N_SITES_PH

driver = DMRGDriver(scratch="./tmp", symm_type=SymmetryTypes.SZ, n_threads=4)
driver.initialize_system(n_sites=L, n_elec=N_ELEC, spin=0)

# [Part A] Set states and matrix representation of operators in local Hilbert space
site_basis, site_ops = [], []
Q = driver.bw.SX # quantum number wrapper (n_elec, 2 * spin, point group irrep)

for k in range(L):
    if k < N_SITES_ELEC:
        # electron part
        basis = [(Q(0, 0, 0), 1), (Q(1, 1, 0), 1), (Q(1, -1, 0), 1), (Q(2, 0, 0), 1)] # [0ab2]
        ops = {
            "": np.array([[1, 0, 0, 0], [0, 1, 0, 0], [0, 0, 1, 0], [0, 0, 0, 1]]), # identity
            "c": np.array([[0, 0, 0, 0], [1, 0, 0, 0], [0, 0, 0, 0], [0, 0, 1, 0]]), # alpha+
            "d": np.array([[0, 1, 0, 0], [0, 0, 0, 0], [0, 0, 0, 1], [0, 0, 0, 0]]), # alpha-
            "C": np.array([[0, 0, 0, 0], [0, 0, 0, 0], [1, 0, 0, 0], [0, -1, 0, 0]]), # beta+
            "D": np.array([[0, 0, 1, 0], [0, 0, 0, -1], [0, 0, 0, 0], [0, 0, 0, 0]]), # beta-
        }
    else:
        # phonon part
        basis = [(Q(0, 0, 0), N_PH)]
        ops = {
            "": np.identity(N_PH), # identity
            "E": np.diag(np.sqrt(np.arange(1, N_PH)), k=-1), # ph+
            "F": np.diag(np.sqrt(np.arange(1, N_PH)), k=1), # ph-
        }
    site_basis.append(basis)
    site_ops.append(ops)

# [Part B] Set Hamiltonian terms in Hubbard-Holstein model
driver.ghamil = driver.get_custom_hamiltonian(site_basis, site_ops)
b = driver.expr_builder()

# electron part
b.add_term("cd", np.array([[i, i + 1, i + 1, i] for i in range(N_SITES_ELEC - 1)]).ravel(), -1)
b.add_term("CD", np.array([[i, i + 1, i + 1, i] for i in range(N_SITES_ELEC - 1)]).ravel(), -1)
b.add_term("cdCD", np.array([[i, i, i, i] for i in range(N_SITES_ELEC)]).ravel(), U)
```

```

# phonon part
b.add_term("EF", np.array([[i + N_SITES_ELEC, ] * 2 for i in range(N_SITES_PH)]).ravel(), OMEGA)

# interaction part
b.add_term("cde", np.array([[i, i, i + N_SITES_ELEC] for i in range(N_SITES_ELEC)]).ravel(), G)
b.add_term("cdf", np.array([[i, i, i + N_SITES_ELEC] for i in range(N_SITES_ELEC)]).ravel(), G)
b.add_term("CDE", np.array([[i, i, i + N_SITES_ELEC] for i in range(N_SITES_ELEC)]).ravel(), G)
b.add_term("CDF", np.array([[i, i, i + N_SITES_ELEC] for i in range(N_SITES_ELEC)]).ravel(), G)

# [Part C] Perform DMRG
mpo = driver.get_mpo(b.finalize(adjust_order=True), algo_type=MPOAlgorithmTypes.FastBipartite)
mps = driver.get_random_mps(tag="KET", bond_dim=250, nroots=1)
energy = driver.dmrg(mpo, mps, n_sweeps=10, bond_dims=[250] * 4 + [500] * 4,
    noises=[1e-4] * 4 + [1e-5] * 4 + [0], thrds=[1e-10] * 8, dav_max_iter=30, iprint=2)
print("DMRG energy = %20.15f" % energy)

```

Listing 1. A Python script to setup the Hubbard-Holstein model Hamiltonian and perform DMRG to find the ground state using BLOCK2. In the script, we use the characters c, d, C, D, E, and F (as an example) to represent the fermionic elementary operators $a_\alpha^\dagger, a_\alpha, a_\beta^\dagger$, and a_β and the bosonic elementary operators b^\dagger and b , respectively. The expected output of this script (the ground state energy) is -6.956893 .

The key to achieving efficiency is to construct MPOs in such a way as to obtain sparse MPO tensors. We note that MPOs contain a gauge degree of freedom and can thus be written in multiple ways, but a sparse representation is typically available as the operators of interest are quite restricted (e.g. of one- and two-particle form). To correctly identify a sparse MPO representation, several ideas have been discussed in the literature.^{40,95,108,109} In BLOCK2, we implement two of them.

(i) The bipartite approach.¹⁰⁹ This is an efficient graph-theory-based approach to build an exact MPO that identifies the best sparse representation. When used with the *ab initio* Hamiltonian, this produces the optimal MPO bond dimension and sparse structure of the matrices, and thus the correct complexity in an *ab initio* DMRG algorithm.

(ii) The singular value decomposition (SVD) approach.^{95,110,111} This approach introduces the possibility of MPO bond dimension compression. For some operators, e.g. *ab initio* Hamiltonians of large molecules, the MPO bond dimension reduction can greatly increase the DMRG efficiency (see Fig. 4). For large numbers of orbitals and/or high-order (more than three-body) terms in the Hamiltonian, the direct SVD of integral matrices can be expensive, and we alleviate this problem by performing SVD for each symmetry block of the MPO tensors separately. Although the SVD does not preserve sparsity, sparsity can be introduced using the sub-Hamiltonian strategy,⁹⁵ which recovers the correct DMRG complexity and MPO tensor sparsity.

Fig. 4 shows a numerical example comparing MPOs resulting from different constructions.

D. MPO/MPS algebra

The MPO and MPS representation of operators and states allow one to view DMRG algorithms in a very general sense as an extension of linear algebra.⁹⁵ BLOCK2 supports this general perspective with a convenient inter-

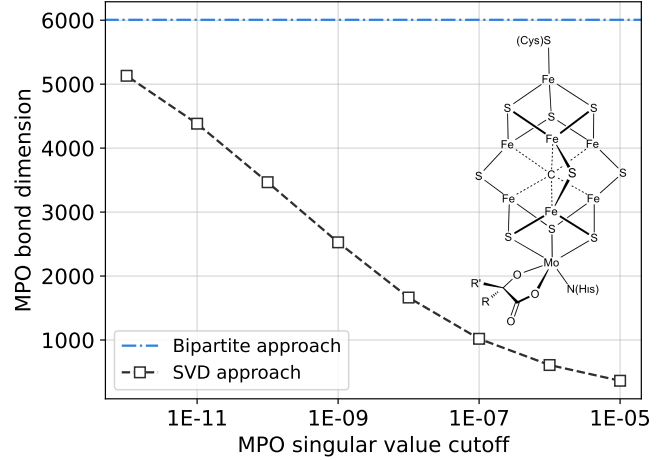


FIG. 4. A comparison between the MPO bond dimensions for MPOs constructed using the bipartite approach¹⁰⁹ and the SVD approach⁹⁵ with different cutoffs for the singular values, for the (76o, 113e) active space model of the FeMo cofactor.¹¹² The active space model is from Ref. 21.

face to MPO/MPS algebraic operations and algorithms. The interface dispatches at the backend to several implementations for different levels of efficiency.

1. Sweep algorithms for MPO/MPS algebra

Consider a general MPO/MPS algebraic expression

$$|\text{MPS}'\rangle = \text{poly}(\text{MPO})(\alpha|\text{MPS}_1\rangle + \beta|\text{MPS}_2\rangle) \quad (3)$$

where $\text{poly}(\text{MPO})$ (can be a linear combination of powers of an MPO or its inverse), $|\text{MPS}_1\rangle$, and $|\text{MPS}_2\rangle$ are known quantities, and α and β are known scalar numbers. In one MPO/MPS algebra backend, we numerically find $|\text{MPS}'\rangle$ by fitting. Namely, starting from a trial $|\text{MPS}'\rangle$,

we solve the optimization problem

$$\max_{|\text{MPS}'\rangle} \|\langle \text{MPS}' | \text{poly}(\text{MPO})(\alpha|\text{MPS}_1\rangle + \beta|\text{MPS}_2\rangle)\| \quad (4)$$

by updating the tensors in $|\text{MPS}'\rangle$ using the one-site or two-site sweep algorithms. Due to its similarity to the standard DMRG algorithm, this procedure is implemented very efficiently in BLOCK2. The standard caveats of DMRG optimization apply however, namely, there can be a dependence on the initial guess (especially for small bond dimension) and the global optimality of the solution is not guaranteed. Using this approach, BLOCK2 implements the following important primitives of MPO/MPS algebra.

(i) Addition, subtraction, and scalar multiplication of MPS. This is implemented by fitting $|\text{MPS}'\rangle$ to $\alpha|\text{MPS}_1\rangle + \beta|\text{MPS}_2\rangle$.

(ii) Matrix-vector multiplication. This is implemented by fitting $|\text{MPS}'\rangle$ to MPO $|\text{MPS}\rangle$.

(iii) Linear equation or matrix inversion. This can be formally expressed as $|\text{MPS}'\rangle = \text{MPO}^{-1}|\text{MPS}\rangle$. By using sweep algorithms,^{32,103,113} we can transform this equation into an effective linear algebra equation defined on one or two sites of $|\text{MPS}'\rangle$, which can be solved using iterative algorithms such as Conjugate Gradient (CG),¹¹⁴ MINRES,¹¹⁵ GCROT(m, k),¹¹⁶ IDRS,¹¹⁷ Chebyshev,¹¹⁸ and LSQR.¹¹⁹

(iv) Matrix exponentiation. This can be formally expressed as $|\text{MPS}'\rangle = \exp(-\beta \text{MPO})|\text{MPS}\rangle$, and $|\text{MPS}'\rangle$ can be found using the time-dependent DMRG methods described in Section II G 3.

2. Exact algorithms for MPO/MPS algebra

MPO/MPS algebra can also be implemented exactly using block-sparse tensor contraction operations. For typical quantum chemistry problems the bond dimensions of the MPS and MPOs are on the order of several thousand, and intermediates generated by the contraction of MPS and MPO tensors can quickly exceed the available memory. Nevertheless, this scheme can be useful for model Hamiltonians with simpler interactions or for benchmarking purposes.

To support exact MPO/MPS algebra, we provide a separate open source library called PYBLOCK3¹²⁰ which more fully exposes the tensor network view of DMRG algorithms, at some cost to efficiency. In PYBLOCK3, the MPO, MPS, and block-sparse tensor objects can be easily manipulated with an interface similar to performing operations on NUMPY arrays,¹²¹ so that arbitrary MPO/MPS algebra is straightforward. We provide subroutines to translate MPO and MPS objects back and forth between BLOCK2 and PYBLOCK3. Note that we do not currently support SU(2) symmetry in PYBLOCK3, thus this interoperability is only possible for non-spin-adapted objects.

As MPS and MPO are represented as pure Python data structures in PYBLOCK3, users can further explore many other possibilities through the interface between BLOCK2 and PYBLOCK3. For example, utilizing the automatic differentiation¹²² feature implemented in PYBLOCK3, we can perform gradient style optimization of MPO or MPS tensors.

3. Symbolic manipulation and simplification of operator expressions

For algebra involving only fermionic operators, BLOCK2 provides an efficient symbolic engine to manipulate, simplify, and truncate expressions using Wick's theorem.⁷⁶ Compared to other existing similar implementations,¹²³⁻¹²⁹ we provide a user friendly Python interface with support for expressions arising in spin-free, spin unrestricted, and general spin theories. Once the algebraic simplifications have been performed, the resulting symbolic expression can be converted into an MPO using techniques in Section II C. Some examples of applications include:

(i) MPO construction of the normal-ordered \hat{H} . Such MPOs increase the numerical stability in low precision DMRG.

(ii) MPO construction of \hat{H}^2 , used to compute the energy variance of an MPS. (Note that computing the norm of $\hat{H}|\text{MPS}\rangle$ (by first constructing an MPS intermediate of $\hat{H}|\text{MPS}\rangle$ using fitting) is an alternative way to obtain the variance which is also often cheaper).

(iii) MPO construction of $e^{-\hat{T}}\hat{H}e^{\hat{T}}$, which arises in theories involving a similarity transform of the Hamiltonian.⁷⁶ In practice, we first rewrite the expression in terms of nested commutators using the Baker-Campbell-Hausdorff expansion. After simplification (and truncation if necessary) we obtain an expression that can be used to generate the MPO.

Fig. 5 shows a numerical example of DMRG using a similarity transformed Hamiltonian constructed from CC amplitudes.

E. MPS analysis and properties

Once we have computed an MPS (e.g. from the DMRG sweep algorithm) we can analyze it in terms of quantities familiar to standard quantum chemistry. Below, we list some representative quantities that can be extracted from an MPS (or a pair of bra and ket MPSs) in BLOCK2.

1. N -particle reduced density matrices

N -particle density matrices (N -PDMs)^{90,132,133} summarize the information in a wavefunction and have many applications across quantum chemistry, such as in orbital

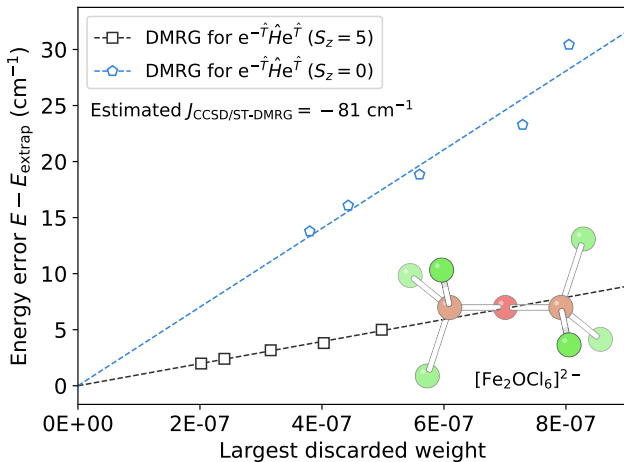


FIG. 5. The extrapolation of DMRG sweep energies using MPS bond dimension $M = 600, 500, 400, 300$, and 200 , for the $(30o, 30e)$ active space of the similarity transformed Hamiltonian $e^{-\hat{T}}\hat{H}e^{\hat{T}}$ with only terms up to three-body interaction kept after normal ordering, computed for the high spin ($S_z = 5$) and low spin ($S_z = 0$) states of the $[\text{Fe}_2\text{OCl}_6]^{2-}$ cluster, using the cc-pVQZ-DK basis and the exact two-component relativistic correction.¹³⁰ The cluster geometry is from Ref. 131.

optimization,^{89,90} (internally) contracted dynamical correlation theories,^{128,133} and so on. In BLOCK2 we provide an efficient algorithm to compute N -PDMs of MPS with arbitrary N (in practice, only $N < 5$ can be computed in non-trivial systems). The implementation has the following features.

(i) We support both N -PDMs (with integer N) and transition N -PDMs (with integer or half-integer N). In a unified framework, the user can compute spin-traced, spin specific, or general spin PDMs.

(ii) The user can freely choose the fermionic operator ordering in the N -PDMs via an operator string input parameter. For example, for the spin-traced 3-PDM, both

$$E_{abcdef}^{(1)} := \sum_{\sigma\tau\lambda} \langle a_{a\sigma}^\dagger a_{b\tau}^\dagger a_{c\lambda}^\dagger a_{d\lambda} a_{e\tau} a_{f\sigma} \rangle \quad (5)$$

and

$$E_{abcdef}^{(2)} := \sum_{\sigma\tau\lambda} \langle a_{a\sigma}^\dagger a_{b\sigma} a_{c\tau}^\dagger a_{d\tau} a_{e\lambda}^\dagger a_{f\lambda} \rangle \quad (6)$$

notations are supported, where the former is compatible with the STACKBLOCK convention,⁵⁹ and the latter is used in the literature of spin-free NEVPT2.¹³⁴

(iii) When obtaining multiple N -PDMs or PDMs with different operator orderings, they can be computed simultaneously within a single sweep so that intermediates can be reused, saving computational time.

(iv) When only a part of the PDM is required (by restricting the indices) we can compute only the required part with a greatly reduced complexity. For example, the

diagonal 2-PDM

$$E_{ppqq} := \sum_{\sigma\tau} \langle a_{p\sigma}^\dagger a_{p\sigma} a_{q\tau}^\dagger a_{q\tau} \rangle \quad (7)$$

required in perturbative DMRG¹⁰⁴ can be computed with a complexity similar to that of the 1-PDM.

(v) We use a hybrid distributed and shared-memory parallelization strategy. For the shared-memory part, we use parallelism over non-redundant collective matrix element indices. For the distributed part, we use a hybrid strategy based on parallelism over sub-operator-strings and parallelism over single matrix element indices.

2. Entanglement analysis

We can compute various entanglement metrics of interest from the MPS.^{37,86,135,136}

(i) One can access the bipartite entanglement entropy^{135,137} in the MPS at each site after a standard DMRG optimization.

(ii) The 1 and 2 orbital DMs³⁷ can be computed using the general N -PDM interface implemented in BLOCK2, with a computational scaling similar to that of the 2-PDM. The mutual information matrix of orbital interactions can be constructed from these ODMs, as a measure of the entanglement between pairs of orbitals.¹³⁶ The mutual information can then be used as the cost function in GA,⁸⁵ to find an optimal orbital ordering for DMRG. Currently this feature is only implemented for non-spin-adapted MPS.

3. Coefficients of configuration state functions or determinants

In quantum chemistry applications, it is useful to understand the determinant or CSF expansion of the DMRG wavefunction (MPS) and these can be computed using **BLOCK2**. In the following we provide some representative use cases:

(i) In BLOCK2, one can extract all CSFs or determinants and their coefficients where the absolute value of the coefficient in the CI expansion is above a given threshold. This uses a depth-first search algorithm performed along the sweep.¹³⁸ When only a few CSFs or determinants satisfy the criterion, the computational cost of this algorithm is almost negligible. From the spin coupling pattern in the dominant CSFs or determinants, one obtains valuable insights into the electronic structure. Currently, for spin-adapted MPS with a non-zero total spin, the algorithm is only implemented for MPS in the singlet-embedding³⁵ format.

(ii) We can use this algorithm to extract the T_3 and T_4 coupled cluster amplitudes, required in externally corrected CCSD¹³⁹ where the DMRG wavefunction is the external source.¹³⁸ For this purpose, we use a much

smaller threshold for the CI coefficient, and an additional restriction on the excitation order (up to quadruples) with respect to the Fermi vacuum to preserve the polynomial complexity of the overall algorithm.

(iii) The same extraction algorithm can also be utilized in a tailored CCSD^{140,141} code using the DMRG wavefunction as the external source for extracting the T_1 and T_2 coupled cluster amplitudes in the active space.^{142,143}

F. MPS transformations

In BLOCK2 the MPS may be converted between different representations suitable for different tasks. There are some limitations on the operations supported in different MPS representations. Below, we discuss examples of such MPS transformations.

1. Singlet embedding

A spin-adapted MPS with non-zero total spin can be represented in either the singlet embedding (SE)^{35,42,53} format (with additional non-interacting fictitious spins added to the end of the DMRG lattice to create a singlet) or the non-singlet-embedding (NSE) format.

For MPS expressed in the SE format, there is no accuracy loss when changing the canonical form between sites, so the DMRG optimization process becomes more stable. However, the SE MPS form makes it difficult to evaluate certain quantities, such as the one-particle triplet transition density matrix (1-TTDM),⁴² required in the 2-step treatment of the SOC effect.⁶⁹ On the other hand, we do not support the computation of CSF coefficients from NSE MPS. To overcome these limitations, we have implemented the exact transformation from SE to NSE MPS, and from NSE to SE MPS. The user can perform the optimization of MPS using either the SE or NSE format, and then transform the MPS to the appropriate format before computing the 1-TTDM or extracting CSF coefficients.

2. Orbital rotations

To improve the representation power of a given bond dimension MPS in DMRG, it is sometimes desirable to rotate the orbital basis.¹⁴⁴ In BLOCK2 we use an exponential parametrization of the orbital rotation matrix,¹⁴⁵ and implement the orbital rotation as a time evolution.^{31,103} As an example usage of this transformation, one can perform DMRG optimization using a set of localized orbitals, and then compute the determinant coefficients defined in a different set of orbitals after an MPS orbital rotation.

As the MPS entanglement structure in two sets of orbitals can be significantly different, often the MPS orbital rotation cannot be performed exactly. When a fixed bond

dimension and time step is used for the transformation, the resulting MPS can sometimes be highly inaccurate. We provide a few additional options to improve the accuracy.

(i) When we want the orbital transformation to approximately preserve the orbital ordering, we use the Kuhn-Munkres algorithm^{146,147} to first match the old and new orbitals.

(ii) We can remove some artificial rotations in the logarithm of the rotation matrix by forcing all leading principal minors of the rotation matrix to be non-negative.

3. Symmetry mappings

As described earlier, BLOCK2 supports many kinds of symmetries in the DMRG calculations. We also provide the ability to transform MPS from a higher to a lower symmetry group. For example:

(i) We can transform spin-adapted (SA) MPS^{35,39,41} to non-spin-adapted (NSA) MPS. This can be done exactly, and the bond dimension of the transformed NSA MPS will generally be higher than that of the SA MPS.³⁵ Since the DMRG optimization of the SA MPS is often much cheaper, this can be useful when the analysis has to be performed on the NSA MPS (for example, when information on the determinant expansion is desired). When the SA MPS is not a singlet, the user can additionally set the desired projected spin of the transformed NSA MPS, and the transformed MPS will have both well-defined total and projected spin.

(ii) We can transform from an MPS expressed in one point group to a subgroup. To perform such a transformation, the user must provide a mapping between the irreducible representations in the two groups. In BLOCK2 we implement this type of MPS symmetry mapping using a fitting approach, where a small fitting error can be expected.

G. DMRG for dynamical and time-dependent quantities

BLOCK2 supports a full suite of algorithms to compute dynamical quantities, such as Green's functions, as well as to perform time-dependent state propagation.

1. Dynamical DMRG

Dynamical DMRG (DDMRG) is the original extension of the standard DMRG algorithm to compute dynamical quantities, such as Green's functions and other spectroscopic quantities^{32,103,148–150} [we will use the electron removal (IP) part of one-particle Green's function in the examples below]. In BLOCK2, we provide an improved version of dynamical DMRG called DDMRG⁺⁺, introduced in Ref. 103. We provide the following options for this method.

(i) We can solve the response equations to find the correction vector as an MPS, and the IP one-particle Green's function is obtained as the expectation value

$$G_{ij}^-(\omega) := \langle \Psi_0 | a_j^\dagger | \Psi_i'(\omega) \rangle \quad (8)$$

$$[\hat{H}_0 - E_0 + \omega - i\eta] |\Psi_i'(\omega)\rangle = a_i |\Psi_0\rangle \quad (9)$$

where $|\Psi_0\rangle$ and E_0 are the (assumed real) ground state MPS and energy, $|\Psi_i'(\omega)\rangle$ is the correction vector MPS, $G_{ij}^-(\omega)$ is the IP part of one-particle Green's function, and ω and η are the real frequency and broadening factor, respectively. In general, $|\Psi_i'(\omega)\rangle$ will be complex, and we solve this equation in the complex domain using the DDMRG⁺⁺ sweep algorithm.

(ii) Alternatively, we write the correction vector as $|\Psi_i'(\omega)\rangle := |X_i(\omega)\rangle + i|Y_i(\omega)\rangle$ and Eq. (9) becomes^{32,103}

$$[(\hat{H}_0 - E_0 + \omega)^2 + \eta^2] |Y_i(\omega)\rangle = \eta a_i |\Psi_0\rangle \quad (10)$$

In BLOCK2 we also use DDMRG⁺⁺ to solve the above equation in the real domain.

(iii) For very small η , both Eq. (9) and Eq. (10) will become ill-conditioned for some ω , and the required number of CG or GCROT¹¹⁶ iterations at each site during the sweep can become large.¹⁵¹ To accelerate the computation of the DMRG Green's function, we support a multi-grid frequency strategy. At the coarse-grained level, we use a large η_0 and a coarse grid of ω_0 for the DDMRG sweeps. At the fine-grained level, we solve Eq. (9) or Eq. (10) using a smaller η only in the middle site in the sweep, for a few ω near the ω_0 value. This method assumes that the renormalized basis in the correction vector MPS generated at ω_0 with a large broadening can be reused for adjacent frequencies. Using this strategy, we can often achieve a good balance between accuracy and efficiency.

2. Chebyshev DMRG

To avoid solving the ill-conditioned response equation in DDMRG, we have also implemented the Chebyshev DMRG approach,^{152–155} based on the Chebyshev expansion of the resolvent and the MPS representation of the Chebyshev vectors.

3. Time-dependent DMRG

BLOCK2 implements time-dependent DMRG (td-DMRG) for true non-equilibrium dynamics, as well as to simulate linear spectra (via the Fourier transform of the autocorrelation function).

(i) We support both imaginary time evolution (ITE) and real time evolution (RTE). When the Hamiltonian is real (and the initial state is real) ITE can be performed using only real arithmetic, while RTE can be carried out in hybrid real-and-complex mode, where the MPO

and rotation matrices in the MPS are represented as real objects, and the MPS tensor at the canonical center is complex. Alternatively, one can perform time evolution where both MPO and MPS are complex and the time step can also be a complex number.

(ii) For the sweep algorithm used in td-DMRG, we implemented both the time-step targeting (TST) approach³¹ and the time-dependent variational principle^{149,156–159} approach. For the TST approach, we support both the td-DMRG and td-DMRG⁺⁺¹⁰³ variants. The Hamiltonian involved in these algorithms can be Hermitian or non-Hermitian (the latter appears when time evolution is used to perform orbital rotation).

Fig. 6 shows a numerical example using time-dependent DMRG.

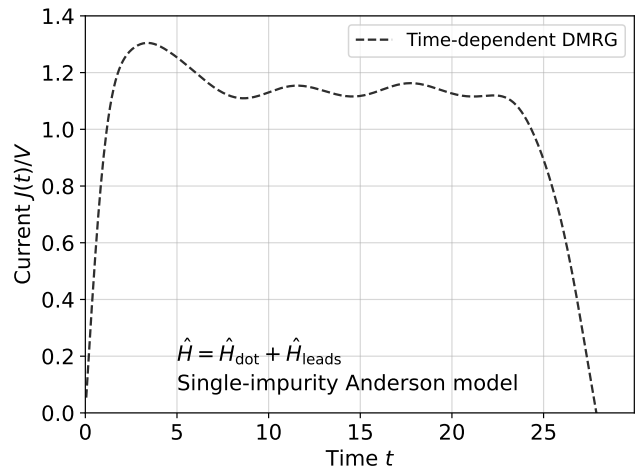


FIG. 6. Current as a function of time for the single impurity Anderson model with $U = 0.5t$, $t' = 0.3535t$, $V = 2U$, $V_g = -0.5U$ and 48 sites, simulated using time-dependent DMRG with the time-dependent variational principle approach, time step $\Delta t = 0.025$, and MPS bond dimension $M = 1000$. (The curve is chosen to illustrate dynamics rather than full convergence with respect to all parameters.) Model parameters are taken from Ref. 160.

H. Finite-temperature DMRG

BLOCK2 supports several finite-temperature DMRG algorithms.

1. Ancilla approach

In the ancilla approach for finite temperature,²⁸ we perform imaginary time evolution of a purified thermal state in an enlarged Hilbert space. Within the context of DMRG, we represent the purified state as an MPS, where ancilla sites are added as a bath. In BLOCK2 we provide subroutines to create the initial finite-temperature MPS at inverse temperature $\beta = 0$ and the finite-temperature

MPO, which is a normal MPO decorated with identity operators at the ancilla sites. We support the evaluation of free energies and PDMs of the finite-temperature MPS by tracing out the ancilla sites. The finite-temperature variants of dynamical DMRG¹⁶¹ and time-dependent DMRG^{162,163} are also available to compute dynamical quantities.

Fig. 7 shows a numerical example of the finite-temperature DMRG using the ancilla approach.

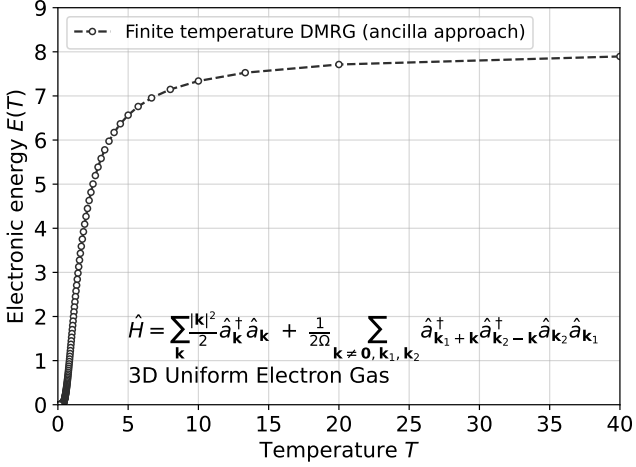


FIG. 7. Electronic energy at different temperatures for the three dimensional uniform electron gas model¹⁶⁴ with density $r_s = 4$, box length $L = 10.24$, and plane wave basis set kinetic energy cutoff $E_{\text{cut}} = 0.6199$, simulated using finite-temperature DMRG with the ancilla approach²⁸ and RK4 for imaginary time evolution,³¹ at chemical potential $\mu = -2$.

2. Sum-over-states approach

To compute properties at very low temperatures (namely, when β is large), the ancilla approach can be inefficient since a large number of time steps is required and this can also generate large entanglement between the physical and ancillary degrees of freedom. We instead perform time-independent DMRG to find a few low-lying eigenstates, and the finite-temperature effects are then computed through a partition function sum over these states. Since the low-lying states can have different particle numbers and spins, we can either represent them using a single particle-number-non-conserving state-averaged MPS, so that the required number of states in each symmetry sector can be determined automatically, or by using multiple state-averaged MPSs to cover all symmetry sectors. The latter scheme may be more efficient, but requires the knowledge of the number of low-energy states in each symmetry sector.

I. DMRG and dynamical correlation

When simulating realistic chemical problems, the number of correlated orbitals can quickly exceed the capabilities of the standard DMRG algorithm for quantum chemistry. Thus it is necessary to combine DMRG with other ideas to treat both static and dynamic correlation effects.^{26,27,126,133,165–171} In the following we list a few different dynamical correlation treatments implemented in BLOCK2.

1. Perturbative DMRG

In perturbative DMRG,¹⁷² the energy of a small bond dimension variational DMRG calculation is corrected using second-order perturbation theory, where the Hamiltonian is partitioned similarly to the Epstein-Nesbet partitioning. In BLOCK2, we include two implementations of this method (for both non-spin-adapted DMRG and spin-adapted DMRG).

(i) In the deterministic perturbative DMRG approach,¹⁷² the first-order perturbative wavefunction is represented as an MPS, which is optimized by solving the response equation using dynamical DMRG (without frequency).

(ii) In the stochastic perturbative DMRG approach,¹⁰⁴ we first compress the first-order wavefunction to a low bond dimension MPS, then the second-order energy correction is evaluated by determinant or CSF sampling.

2. Uncontracted dynamical correlation theories

It is natural to add dynamical correlation to DMRG in the framework of multireference theories, where the DMRG-CASSCF solution is used as a reference state, and low-order excitations from this space are used for the dynamic correlation treatment. We can represent the wavefunction ansatz (including the active, core, and virtual sub-spaces) as an MPS that approximates an uncontracted correlation ansatz.^{113,173} As introduced in a recent report,⁵⁷ we provide a few different implementations to represent and optimize MPS for uncontracted dynamical correlation theories.

(i) We can construct a conventional MPS that describes all the orbital spaces, but restrict the quantum numbers to limit the excitation order out of the active space.⁵⁷ This approach can be trivially supported in BLOCK2, so it is automatically compatible with many other features. However, its efficiency can be low. When the excitation order is restricted to singles, we provide an accelerated solver that bypasses the sweep iterations over the external orbitals.¹⁷⁴

(ii) For improved efficiency, we can introduce two large sites in the MPS to describe the core and virtual spaces so that operations on these orbitals can be handled

specially.⁵⁷ In **BLOCK2**, we support several different treatments of the large site. The CSF and determinant based large-site implementation provides the highest efficiency, for the spin-adapted and non-spin-adapted cases, respectively. We also support building a large-site MPO tensor by contracting normal MPO tensors, which is less efficient.

Using the large-site scheme, we can optimize the MPS energy for different multireference theories (with large active spaces and many core orbitals),⁵⁷ including arbitrary-order multi-reference configuration interaction (MRCI)^{57,175} and size-extensivity corrections,¹⁶⁵ arbitrary-order averaged quadratic coupled cluster (AQCC),¹⁷⁶ arbitrary-order coupled pair functional (ACPF),¹⁷⁷ and arbitrary-order NEVPT^{134,178,179} and restraining the excitation degree multireference perturbation theory (MRREPT).^{168,180,181} Our flexible implementation further allows for the inclusion of arbitrary determinants/CSFs in a fashion similar to selected configuration interaction.

3. Internally contracted dynamical correlations

Internally contracted dynamical correlation theories form a second common framework for multireference correlation. When the active space indices in the excitation operator are also contracted, the corresponding theories are called strongly-contracted.^{80,133,182} Currently we provide the spin-free implementations of fully internally contracted MRCI singles and doubles (FIC-MRCISD),^{126,128} internally contracted NEVPT2,¹⁷⁴ and strongly contracted NEVPT2¹³³ using automatic symbolic expression derivation and DMRG N -PDMs implemented in **BLOCK2**. Other internally contracted theories are supported via the interface between **BLOCK2** and some external packages, which will be discussed in the next section.

Fig. 8 shows a numerical example of the performance of theories for DMRG with dynamical correlations.

III. INTERFACES AND EXTENSIONS

To extend the range of application of DMRG algorithms, we have designed **BLOCK2** to be interoperable with other libraries. In this section, we list some of the available basic interfaces of **BLOCK2**, as well as the interfaces between **BLOCK2** and external packages.

A. Basic interfaces to **block2**

The source code of **BLOCK2** is mainly written in C++11, as a header-only library. We use templates extensively for a concise treatment of different symmetry classes and floating point number types. The code can be compiled using GNU gcc, clang, Apple clang, Intel

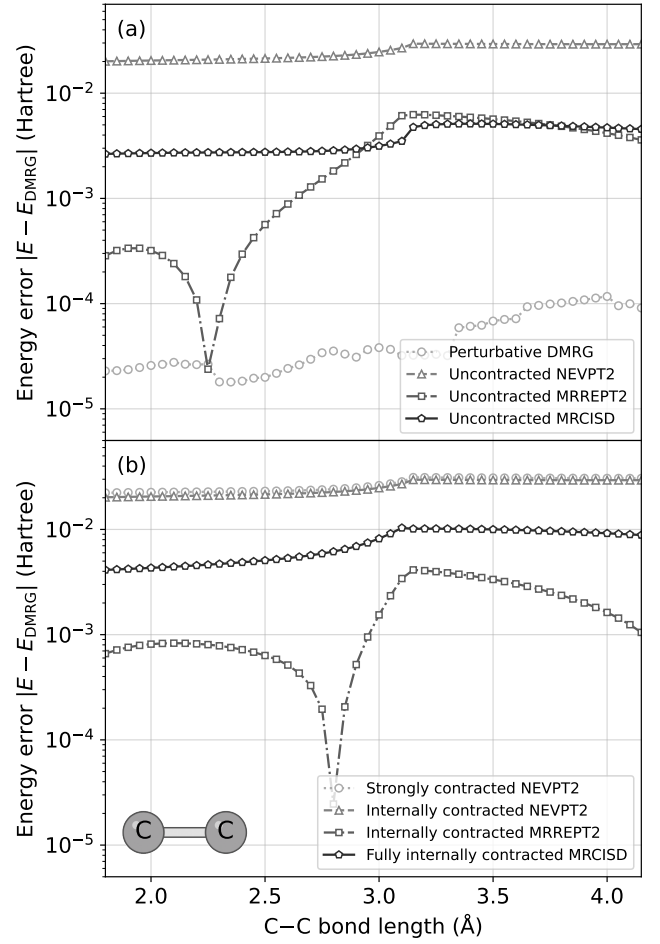


FIG. 8. A comparison between absolute energies computed using DMRG (with MPS bond dimension $M = 3000$) and (a) perturbative DMRG and uncontracted and (b) internally contracted dynamic correlation multi-reference theories implemented in **BLOCK2**, for carbon dimer in the cc-pVDZ basis set at different bond lengths. DMRG-CASSCF with a active space (8o, 8e) is performed to generate the reference state for MRCISD, NEVPT2, and MRREPT2. The reference state for perturbative DMRG is an MPS with $M = 200$.

icc, or the msvc compilers, and supports the Linux, Mac OS, and Windows platforms. For Mac OS we support both the x86 and arm64 instruction architectures. Currently, development and testing focus on the Linux (x86) and Mac OS (x86) platforms. We currently provide the following basic interfaces to **BLOCK2**.

(i) A Python library interface to **block2** and **pyblock2** (not to be confused with **pyblock3**). The former exposes almost all C++ classes and functions to Python using PYBIND11.¹⁸³ The latter provides some helper and driver classes written in pure Python, for users to easily customize their workflow.

(ii) The Python script **block2main** for parsing input files and to run DMRG. This provides a simple interface which should be familiar to users of conventional quan-

tum chemistry packages. The input file format is also compatible with that of **STACKBLOCK**,⁵⁹ so existing applications that call **STACKBLOCK** as an executable can be directly used with **BLOCK2**. A list of the supported keywords is given in the documentation.

(iii) A C++ executable **block2** to parse input files and run DMRG. We have found this interface to be useful when performing very large scale distributed parallel computations, where the Python components can induce significant overheads.

(iv) The C++ library **block2.so**, which can be used together with other packages written in C++. In principle, one can also simply include **BLOCK2** header files in a C++ project without linking to the library. However, in practice this may introduce unnecessary extra compilation time.

Besides providing freely downloadable source code, we also provide precompiled packages for the Python interfaces, which can be installed using `pip install block2` [without the Message Passing Interface (MPI) library dependence] or `pip install block2-mpi` (with MPI dependence).

B. Extension interfaces to external packages

We provide the following interfaces to external packages to extend the functionality of **BLOCK2**.

(i) **PySCF**.^{49,50} The orbitals and integrals required for running DMRG can be computed using mean-field methods implemented in **PySCF**. One can also perform DMRG-CASSCF (energy and gradients),⁹⁰ DMRG SC-NEVPT2 (using the exact 4PDM¹³³ or MPS compression⁸⁰) with **PySCF** and **BLOCK2** (this partially reuses the existing **PySCF** interface to **STACKBLOCK**, which gives an alternative implementation of SC-NEVPT2 to the native implementation in **BLOCK2**). Using the Python interface to the **BLOCK2** symbolic engine and some of the **PySCF** infrastructure, one can also automatically derive and implement a variety of coupled cluster theories.

(ii) **LIBDMET**.¹⁸⁴ One can use ground state or finite temperature DMRG as the impurity solver¹⁸⁵ for *ab initio* Density Matrix Embedding Theory (DMET) through the interface between **BLOCK2** and **LIBDMET**.¹⁸⁶ In particular, the *ab initio* DMRG with general spin orbitals was implemented as an impurity solver for the superconducting Hamiltonian.¹⁸⁷

(iii) **FCDMFT**.^{188,189} One can use dynamical DMRG or DMRG uncontracted MRCI as the impurity solver for *ab initio* full cell Dynamical Mean-Field Theory (DMFT) using **BLOCK2** with **FCDMFT**.

(iv) **STACKBLOCK**.^{35,59} We provide scripts to transform MPSs (in both directions) between **STACKBLOCK** and **BLOCK2**. This is primarily useful for benchmarking purposes.

(v) **PYBLOCK3**.¹²⁰ We provide scripts to transform MPSs and MPOs in both directions between **PYBLOCK3**

and **BLOCK2**.

(vi) **OPENMOLCAS**.¹⁹⁰ We can perform DMRG-CASSCF and DMRG-CASPT2^{167,191–193} (with or without cumulant approximations¹⁹⁴) using **OPENMOLCAS** and **BLOCK2**. This is implemented using a small modification to the existing interface between **OPENMOLCAS** and **STACKBLOCK**.¹⁹⁵

(vii) **FORTE**.¹⁹⁶ One can perform DMRG-CASCI, DMRG-CASSCF, and DMRG-Driven-Similarity-Renormalization-Group (DSRG)¹⁷¹ with the interface between **FORTE** and **BLOCK2**.

(viii) **QISKit**.¹⁹⁷ Through the Python interface in **BLOCK2** one can perform fermionic or spin DMRG for Hamiltonian expressions generated in **QISKit**. For example, one can perform fermionic DMRG from the **QISKit** second quantized Hamiltonian expression, or DMRG for Hamiltonians expressed as linear combinations of arbitrary-length Pauli strings.⁸³

As suggested by these examples, it is also simple to extend **BLOCK2** interfaces to work with many other packages.

IV. CONCLUSIONS

After more than three years of development, the robustness, utility, and comprehensiveness of the **BLOCK2** framework has been examined and tested across a great variety of projects. In our experience, the range of implementations and algorithms provided by **BLOCK2** has allowed DMRG to be fruitfully applied for many different purposes, ranging from benchmarking other methods, to obtaining high-accuracy definitive results in *ab initio* and model simulations. Moving forwards, we will continue to develop **BLOCK2** as an open framework for DMRG algorithms and to further extend its integration with other packages. We hope that **BLOCK2** will serve as platform to extend DMRG to new domains and to generate insights into new scientific areas.

ACKNOWLEDGMENTS

H.Z. thanks Sandeep Sharma for helpful discussions. This framework was produced over several years with contributions from multiple individuals. Work by H.Z. was supported by the US National Science Foundation, under Award no. CHE-2102505. Work by H.R.L. and T.Z. was supported by the Air Force Office of Scientific Research, under Award FA9550-18-1-0095. H.R.L. acknowledges support from a postdoctoral fellowship from the German Research Foundation (DFG) via grant LA 4442/1-1 during the first part of this work. Work by S.L. (this material) was supported by the US Department of Energy, Office of Science, National Quantum Information Science Research Centers, Quantum Systems Accelerator. Work by Z.C. was supported by the US Department of Energy, Office of Science, under Award No.

DE-SC0018140. Work by C.S. was supported by the US Department of Energy, Office of Science, under Grant No. DE-SC0019374. Work by L.P. was supported by the US Department of Energy, Office of Science, via the M2QM EFRC under Grant No. DE-SC0019330. Work by R.P. was supported by the US National Science Foundation, under Award no. CHE-2102505. Work by K.L. was supported by the US Department of Energy, Office of Science, Basic Energy Sciences and Office of Advanced Scientific Computing Research, Scientific Discovery through Advanced Computing (SciDAC) program, under Award No. DE-SC0022088. Work by J.T. was supported by the US Department of Energy, Office of Science, under Award No. DE-SC0018140. J.T. acknowledges funding through a postdoctoral research fellowship from the Deutsche Forschungsgemeinschaft (DFG, German Research Foundation)-495279997. Work by J.Y. was supported by the US Department of Energy, Office of Science, via the M2QM EFRC under Grant No. DE-SC0019330. The computations presented in this work were conducted at the Resnick High Performance Computing Center, a facility supported by the Resnick Sustainability Institute at the California Institute of Technology.

DATA AVAILABILITY

The reference input and output files for producing data in the numerical examples can be found in the GitHub repository <https://github.com/hczhai/block2-example-data>. The reference software version is BLOCK2 0.5.2.

¹White, S. R. Density matrix formulation for quantum renormalization groups. *Physical Review Letters* **1992**, *69*, 2863.

²White, S. R. Density-matrix algorithms for quantum renormalization groups. *Physical Review B* **1993**, *48*, 10345.

³Verstraete, F.; Nishino, T.; Schollwöck, U.; Bañuls, M. C.; Chan, G. K.; Stoudenmire, M. E. Density matrix renormalization group, 30 years on. *Nature Reviews Physics* **2023**, *1*, 4.

⁴Hachmann, J.; Cardoen, W.; Chan, G. Multireference correlation in long molecules with the quadratic scaling density matrix renormalization group. *The Journal of Chemical Physics* **2006**, *125*, 144101–144101.

⁵Singh, S.; Zhou, H.-Q.; Vidal, G. Simulation of one-dimensional quantum systems with a global SU(2) symmetry. *New Journal of Physics* **2010**, *12*, 033029.

⁶LeBlanc, J. P.; Antipov, A. E.; Becca, F.; Bulik, I. W.; Chan, G. K.-L.; Chung, C.-M.; Deng, Y.; Ferrero, M.; Henderson, T. M.; Jiménez-Hoyos, C. A., et al. Solutions of the two-dimensional Hubbard model: Benchmarks and results from a wide range of numerical algorithms. *Physical Review X* **2015**, *5*, 041041.

⁷Motta, M.; Ceperley, D. M.; Chan, G. K.-L.; Gomez, J. A.; Gull, E.; Guo, S.; Jiménez-Hoyos, C. A.; Lan, T. N.; Li, J.; Ma, F., et al. Towards the solution of the many-electron problem in real materials: Equation of state of the hydrogen chain with state-of-the-art many-body methods. *Physical Review X* **2017**, *7*, 031059.

⁸Motta, M.; Genovese, C.; Ma, F.; Cui, Z.-H.; Sawaya, R.; Chan, G. K.-L.; Chepiga, N.; Helms, P.; Jiménez-Hoyos, C.; Millis, A. J., et al. Ground-state properties of the hydrogen chain: dimerization, insulator-to-metal transition, and magnetic phases. *Physical Review X* **2020**, *10*, 031058.

⁹Hachmann, J.; Dorando, J. J.; Avilés, M.; Chan, G. K.-L. The radical character of the acenes: A density matrix renormalization group study. *The Journal of Chemical Physics* **2007**, *127*, 134309.

¹⁰Marti, K. H.; Ondik, I. M.; Moritz, G.; Reiher, M. Density matrix renormalization group calculations on relative energies of transition metal complexes and clusters. *The Journal of Chemical Physics* **2008**, *128*, 014104–014104.

¹¹Kurashige, Y.; Yanai, T. High-performance ab initio density matrix renormalization group method: Applicability to large-scale multireference problems for metal compounds. *The Journal of Chemical Physics* **2009**, *130*, 234114–234114.

¹²Mizukami, W.; Kurashige, Y.; Yanai, T. Communication: Novel quantum states of electron spins in polycarbene from ab initio density matrix renormalization group calculations. *The Journal of Chemical Physics* **2010**, *133*, 091101.

¹³Kurashige, Y.; Chan, G. K.-L.; Yanai, T. Entangled quantum electronic wavefunctions of the Mn_4CaO_5 cluster in photosystem II. *Nature Chemistry* **2013**, *5*, 660–666.

¹⁴Harris, T. V.; Kurashige, Y.; Yanai, T.; Morokuma, K. Ab initio density matrix renormalization group study of magnetic coupling in dinuclear iron and chromium complexes. *The Journal of Chemical Physics* **2014**, *140*, 054303.

¹⁵Sharma, S.; Sivalingam, K.; Neese, F.; Chan, G. K.-L. Low-energy spectrum of iron–sulfur clusters directly from many-particle quantum mechanics. *Nature Chemistry* **2014**, *6*, 927–933.

¹⁶Chalupsky, J.; Rokob, T. A.; Kurashige, Y.; Yanai, T.; Solomon, E. I.; Rulisek, L.; Srnec, M. Reactivity of the binuclear non-heme iron active site of Δ^9 desaturase studied by large-scale multireference ab initio calculations. *Journal of the American Chemical Society* **2014**, *136*, 15977–15991.

¹⁷Li, Z.; Guo, S.; Sun, Q.; Chan, G. K.-L. Electronic landscape of the P-cluster of nitrogenase as revealed through many-electron quantum wavefunction simulations. *Nature Chemistry* **2019**, *11*, 1026–1033.

¹⁸Larsson, H. R.; Zhai, H.; Umrigar, C. J.; Chan, G. K.-L. The chromium dimer: closing a chapter of quantum chemistry. *Journal of the American Chemical Society* **2022**, *144*, 15932–15937.

¹⁹Frahm, L.-H.; Pfannkuche, D. Ultrafast ab initio quantum chemistry using matrix product states. *Journal of Chemical Theory and Computation* **2019**, *15*, 2154–2165.

²⁰Baiardi, A. Electron dynamics with the time-dependent density matrix renormalization group. *Journal of Chemical Theory and Computation* **2021**, *17*, 3320–3334.

²¹Li, Z.; Li, J.; Dattani, N. S.; Umrigar, C.; Chan, G. K.-L. The electronic complexity of the ground-state of the FeMo cofactor of nitrogenase as relevant to quantum simulations. *The Journal of chemical physics* **2019**, *150*, 024302.

²²Lee, S.; Lee, J.; Zhai, H.; Tong, Y.; Dalzell, A. M.; Kumar, A.; Helms, P.; Gray, J.; Cui, Z.-H.; Liu, W., et al. Evaluating the evidence for exponential quantum advantage in ground-state quantum chemistry. *Nature Communications* **2023**, *14*, 1952.

²³Chan, G. K.-L.; Sharma, S. The density matrix renormalization group in quantum chemistry. *Annual Review of Physical Chemistry* **2011**, *62*, 465–481.

²⁴Wouters, S.; Van Neck, D. The density matrix renormalization group for ab initio quantum chemistry. *The European Physical Journal D* **2014**, *68*, 1–20.

²⁵Baiardi, A.; Reiher, M. The density matrix renormalization group in chemistry and molecular physics: Recent developments and new challenges. *The Journal of Chemical Physics* **2020**, *152*, 040903.

²⁶Yanai, T.; Kurashige, Y.; Mizukami, W.; Chalupský, J.; Lan, T. N.; Saitow, M. Density matrix renormalization group for ab initio Calculations and associated dynamic correlation methods: A review of theory and applications. *International Journal of Quantum Chemistry* **2015**, *115*, 283–299.

²⁷Cheng, Y.; Xie, Z.; Ma, H. Post-density matrix renormalization group methods for describing dynamic electron correlation with

large active spaces. *The Journal of Physical Chemistry Letters* **2022**, *13*, 904–915.

²⁸Feiguin, A. E.; White, S. R. Finite-temperature density matrix renormalization using an enlarged Hilbert space. *Physical Review B* **2005**, *72*, 220401.

²⁹Stoudenmire, E.; White, S. R. Minimally entangled typical thermal state algorithms. *New Journal of Physics* **2010**, *12*, 055026.

³⁰Roemelt, M. Spin orbit coupling for molecular ab initio density matrix renormalization group calculations: Application to g-tensors. *The Journal of Chemical Physics* **2015**, *143*, 044112.

³¹Feiguin, A. E.; White, S. R. Time-step targeting methods for real-time dynamics using the density matrix renormalization group. *Physical Review B* **2005**, *72*, 020404.

³²Jeckelmann, E. Dynamical density-matrix renormalization-group method. *Physical Review B* **2002**, *66*, 045114.

³³Fishman, M.; White, S.; Stoudenmire, E. The iTensor software library for tensor network calculations. *SciPost Physics Code-bases* **2022**, 004.

³⁴Chan, G. K.-L.; Head-Gordon, M. Highly correlated calculations with a polynomial cost algorithm: A study of the density matrix renormalization group. *The Journal of Chemical Physics* **2002**, *116*, 4462–4476.

³⁵Sharma, S.; Chan, G. Spin-adapted density matrix renormalization group algorithms for quantum chemistry. *The Journal of Chemical Physics* **2012**, *136*, 124121–124121.

³⁶Legeza, Ö.; Röder, J.; Hess, B. Controlling the accuracy of the density-matrix renormalization-group method: The dynamical block state selection approach. *Physical Review B* **2003**, *67*, 125114.

³⁷Boguslawski, K.; Tecmer, P.; Barcza, G.; Legeza, O.; Reiher, M. Orbital entanglement in bond-formation processes. *Journal of Chemical Theory and Computation* **2013**, *9*, 2959–2973.

³⁸Luo, H.-G.; Qin, M.-P.; Xiang, T. Optimizing Hartree-Fock orbitals by the density-matrix renormalization group. *Physical Review B* **2010**, *81*, 235129.

³⁹Wouters, S.; Poelmans, W.; Ayers, P. W.; Van Neck, D. CheMPS2: A free open-source spin-adapted implementation of the density matrix renormalization group for ab initio quantum chemistry. *Computer Physics Communications* **2014**, *185*, 1501–1514.

⁴⁰Keller, S.; Dolfi, M.; Troyer, M.; Reiher, M. An efficient matrix product operator representation of the quantum chemical Hamiltonian. *The Journal of Chemical Physics* **2015**, *143*, 244118.

⁴¹Keller, S.; Reiher, M. Spin-adapted matrix product states and operators. *The Journal of Chemical Physics* **2016**, *144*, 134101.

⁴²Li, Z.; Chan, G. K.-L. Spin-projected matrix product states: Versatile tool for strongly correlated systems. *Journal of Chemical Theory and Computation* **2017**, *13*, 2681–2695.

⁴³Brabec, J.; Brandeis, J.; Kowalski, K.; Xantheas, S.; Leggeza, Ö.; Veis, L. Massively parallel quantum chemical density matrix renormalization group method. *Journal of Computational Chemistry* **2021**, *42*, 534–544.

⁴⁴Xie, Z.; Song, Y.; Peng, F.; Li, J.; Cheng, Y.; Zhang, L.; Ma, Y.; Tian, Y.; Luo, Z.; Ma, H. Kylin 1.0: An ab-initio density matrix renormalization group quantum chemistry program. *Journal of Computational Chemistry* **2023**, *44*, 1316–1328.

⁴⁵Zhai, H.; Larsson, H. R.; Lee, S.; Cui, Z.-H. block2: Efficient MPO implementation of quantum chemistry DMRG. 2023; <https://github.com/block-hczhai/block2-preview>.

⁴⁶Zgid, D.; Nooijen, M. On the spin and symmetry adaptation of the density matrix renormalization group method. *The Journal of Chemical Physics* **2008**, *128*, 014107.

⁴⁷Sharma, S. A general non-Abelian density matrix renormalization group algorithm with application to the C2 dimer. *The Journal of Chemical Physics* **2015**, *142*, 024107.

⁴⁸Li, Z. Time-reversal symmetry adaptation in relativistic density matrix renormalization group algorithm. *The Journal of Chemical Physics* **2023**, *158*.

⁴⁹Sun, Q.; Berkelbach, T. C.; Blunt, N. S.; Booth, G. H.; Guo, S.; Li, Z.; Liu, J.; McClain, J. D.; Sayfutyarova, E. R.; Sharma, S., et al. PySCF: the Python-based simulations of chemistry framework. *Wiley Interdisciplinary Reviews: Computational Molecular Science* **2018**, *8*, e1340.

⁵⁰Sun, Q.; Zhang, X.; Banerjee, S.; Bao, P.; Barbry, M.; Blunt, N. S.; Bogdanov, N. A.; Booth, G. H.; Chen, J.; Cui, Z. H., et al. Recent developments in the PySCF program package. *The Journal of Chemical Physics* **2020**, *153*, 024109.

⁵¹Xiang, T. Density-matrix renormalization-group method in momentum space. *Physical Review B* **1996**, *53*, R10445.

⁵²Zhang, S. SO(4) symmetry of the Hubbard model and its experimental consequences. *International Journal of Modern Physics B* **1991**, *5*, 153–168.

⁵³McCulloch, I. P.; Gulácsi, M. The non-Abelian density matrix renormalization group algorithm. *Europhysics Letters* **2002**, *57*, 852.

⁵⁴Zhai, H.; Lee, S.; Cui, Z.-H.; Cao, L.; Ryde, U.; Chan, G. K.-L. Multireference protonation energetics of a dimeric model of nitrogenase iron-sulfur clusters. *arXiv preprint arXiv:2305.07227* **2023**,

⁵⁵White, S. R. Density matrix renormalization group algorithms with a single center site. *Physical Review B* **2005**, *72*, 180403.

⁵⁶Hubig, C.; McCulloch, I. P.; Schollwöck, U.; Wolf, F. A. Strictly single-site DMRG algorithm with subspace expansion. *Physical Review B* **2015**, *91*, 155115.

⁵⁷Larsson, H. R.; Zhai, H.; Gunst, K.; Chan, G. K.-L. Matrix product states with large sites. *Journal of Chemical Theory and Computation* **2022**, *18*, 749–762.

⁵⁸Dorando, J. J.; Hachmann, J.; Chan, G. K.-L. Targeted excited state algorithms. *The Journal of Chemical Physics* **2007**, *127*, 084109.

⁵⁹Sharma, S.; Chan, G. K.-L. block: the density matrix renormalization group (DMRG) algorithm for quantum chemistry. 2012; <https://github.com/sanshar/StackBlock>.

⁶⁰Larsson, H. R. Computing vibrational eigenstates with tree tensor network states (TTNS). *The Journal of Chemical Physics* **2019**, *151*.

⁶¹Li, Z.; Xiao, Y.; Liu, W. On the spin separation of algebraic two-component relativistic Hamiltonians: Molecular properties. *The Journal of Chemical Physics* **2014**, *141*, 054111.

⁶²Moritz, G.; Wolf, A.; Reiher, M. Relativistic DMRG calculations on the curve crossing of cesium hydride. *The Journal of Chemical Physics* **2005**, *123*, 184105.

⁶³Knecht, S.; Legeza, Ö.; Reiher, M. Communication: Four-component density matrix renormalization group. *The Journal of Chemical Physics* **2014**, *140*, 041101.

⁶⁴Battaglia, S.; Keller, S.; Knecht, S. Efficient relativistic density-matrix renormalization group implementation in a matrix-product formulation. *Journal of Chemical Theory and Computation* **2018**, *14*, 2353–2369.

⁶⁵Hoyer, C. E.; Hu, H.; Lu, L.; Knecht, S.; Li, X. Relativistic Kramers-unrestricted exact-two-component density matrix renormalization group. *The Journal of Physical Chemistry A* **2022**, *126*, 5011–5020.

⁶⁶Dyall, K. G.; Fægri Jr, K. *Introduction to relativistic quantum chemistry*; Oxford University Press, 2007.

⁶⁷Zhai, H.; Chan, G. K.-L. A comparison between the one-and two-step spin-orbit coupling approaches based on the ab initio density matrix renormalization group. *The Journal of Chemical Physics* **2022**, *157*, 164108.

⁶⁸Neese, F. Efficient and accurate approximations to the molecular spin-orbit coupling operator and their use in molecular g-tensor calculations. *The Journal of Chemical Physics* **2005**, *122*, 034107.

⁶⁹Sayfutyarova, E. R.; Chan, G. K.-L. A state interaction spin-orbit coupling density matrix renormalization group method. *The Journal of Chemical Physics* **2016**, *144*, 234301.

⁷⁰Sayfutyarova, E.; Chan, G. Electron paramagnetic resonance g-tensors from state interaction spin-orbit coupling density matrix

renormalization group. *The Journal of Chemical Physics* **2018**, *148*, 184103–184103.

⁷¹Chan, G.; Van Voorhis, T. Density-matrix renormalization-group algorithms with nonorthogonal orbitals and non-Hermitian operators, and applications to polyenes. *The Journal of Chemical Physics* **2005**, *122*, 204101.

⁷²White, S. R. Numerical canonical transformation approach to quantum many-body problems. *The Journal of Chemical Physics* **2002**, *117*, 7472–7482.

⁷³Yanai, T.; Chan, G. K.-L. Canonical transformation theory for multireference problems. *The Journal of Chemical Physics* **2006**, *124*, 194106.

⁷⁴Neuscamman, E.; Yanai, T.; Chan, G. K.-L. Strongly contracted canonical transformation theory. *The Journal of Chemical Physics* **2010**, *132*, 024106.

⁷⁵Yanai, T.; Kurashige, Y.; Neuscamman, E.; Chan, G. K.-L. Extended implementation of canonical transformation theory: parallelization and a new level-shifted condition. *Physical Chemistry Chemical Physics* **2012**, *14*, 7809–7820.

⁷⁶Bartlett, R. J.; Musial, M. Coupled-cluster theory in quantum chemistry. *Reviews of Modern Physics* **2007**, *79*, 291.

⁷⁷Mitrushenkov, A.; Fano, G.; Linguerri, R.; Palmieri, P. On the possibility to use non-orthogonal orbitals for Density Matrix Renormalization Group calculations in Quantum Chemistry. *arXiv preprint arXiv:cond-mat/0306058* **2003**,

⁷⁸Liao, K.; Zhai, H.; Christlmaier, E. M.; Schraivogel, T.; Rfos, P. L.; Kats, D.; Alavi, A. Density Matrix Renormalization Group for Transcorrelated Hamiltonians: Ground and Excited States in Molecules. *Journal of Chemical Theory and Computation* **2023**, *19*, 1734–1743.

⁷⁹Baiardi, A.; Reiher, M. Transcorrelated density matrix renormalization group. *The Journal of Chemical Physics* **2020**, *153*, 164115.

⁸⁰Sokolov, A. Y.; Guo, S.; Ronca, E.; Chan, G. K.-L. Time-dependent N-electron valence perturbation theory with matrix product state reference wavefunctions for large active spaces and basis sets: Applications to the chromium dimer and all-trans polyenes. *The Journal of Chemical Physics* **2017**, *146*, 244102.

⁸¹Moritz, G.; Hess, B. A.; Reiher, M. Convergence behavior of the density-matrix renormalization group algorithm for optimized orbital orderings. *The Journal of Chemical Physics* **2005**, *122*, 024107.

⁸²Ma, Y.; Ma, H. Assessment of various natural orbitals as the basis of large active space density-matrix renormalization group calculations. *The Journal of Chemical Physics* **2013**, *138*, 224105.

⁸³Mishmash, R. V.; Gujarati, T. P.; Motta, M.; Zhai, H.; Chan, G. K.-L.; Mezzacapo, A. Hierarchical Clifford Transformations to Reduce Entanglement in Quantum Chemistry Wave Functions. *Journal of Chemical Theory and Computation* **2023**,

⁸⁴Fiedler, M. A property of eigenvectors of nonnegative symmetric matrices and its application to graph theory. *Czechoslovak Mathematical Journal* **1975**, *25*, 619–633.

⁸⁵Olivares-Amaya, R.; Hu, W.; Nakatani, N.; Sharma, S.; Yang, J.; Chan, G. K.-L. The ab-initio density matrix renormalization group in practice. *The Journal of chemical physics* **2015**, *142*, 034102.

⁸⁶Rissler, J.; Noack, R. M.; White, S. R. Measuring orbital interaction using quantum information theory. *Chemical Physics* **2006**, *323*, 519–531.

⁸⁷Sun, Q.; Yang, J.; Chan, G. K.-L. A general second order complete active space self-consistent-field solver for large-scale systems. *Chemical Physics Letters* **2017**, *683*, 291–299.

⁸⁸Smith, J. E.; Lee, J.; Sharma, S. Near-exact nuclear gradients of complete active space self-consistent field wave functions. *The Journal of Chemical Physics* **2022**, *157*, 094104.

⁸⁹Zgid, D.; Nooijen, M. The density matrix renormalization group self-consistent field method: Orbital optimization with the density matrix renormalization group method in the active space. *The Journal of Chemical Physics* **2008**, *128*, 144116.

⁹⁰Ghosh, D.; Hachmann, J.; Yanai, T.; Chan, G. K.-L. Orbital optimization in the density matrix renormalization group, with applications to polyenes and β -carotene. *The Journal of Chemical Physics* **2008**, *128*, 144117–144117.

⁹¹Yanai, T.; Kurashige, Y.; Ghosh, D.; Chan, G. K.-L. Accelerating convergence in iterative solution for large-scale complete active space self-consistent-field calculations. *International Journal of Quantum Chemistry* **2009**, *109*, 2178–2190.

⁹²Hu, W.; Chan, G. K.-L. Excited-state geometry optimization with the density matrix renormalization group, as applied to polyenes. *Journal of Chemical Theory and Computation* **2015**, *11*, 3000–3009.

⁹³Iino, T.; Shiozaki, T.; Yanai, T. Algorithm for analytic nuclear energy gradients of state averaged DMRG-CASSCF theory with newly derived coupled-perturbed equations. *The Journal of Chemical Physics* **2023**, *158*.

⁹⁴Zhai, H.; Chan, G. K.-L. Low communication high performance ab initio density matrix renormalization group algorithms. *The Journal of Chemical Physics* **2021**, *154*, 224116.

⁹⁵Chan, G. K.-L.; Keselman, A.; Nakatani, N.; Li, Z.; White, S. R. Matrix product operators, matrix product states, and ab initio density matrix renormalization group algorithms. *The Journal of chemical physics* **2016**, *145*, 014102.

⁹⁶Stoudenmire, E.; White, S. R. Real-space parallel density matrix renormalization group. *Physical Review B* **2013**, *87*, 155137.

⁹⁷Chen, F.-Z.; Cheng, C.; Luo, H.-G. Real-space parallel density matrix renormalization group with adaptive boundaries. *Chinese Physics B* **2021**, *30*, 080202.

⁹⁸Chan, G. K.-L. An algorithm for large scale density matrix renormalization group calculations. *The Journal of Chemical Physics* **2004**, *120*, 3172–3178.

⁹⁹Levy, R.; Solomonik, E.; Clark, B. K. Distributed-memory DMRG via sparse and dense parallel tensor contractions. *arXiv preprint arXiv:2007.05540* **2020**,

¹⁰⁰Hager, G.; Jeckelmann, E.; Fehske, H.; Wellein, G. Parallelization strategies for density matrix renormalization group algorithms on shared-memory systems. *Journal of Computational Physics* **2004**, *194*, 795–808.

¹⁰¹Eriksen, J. J.; Anderson, T. A.; Deustua, J. E.; Ghanem, K.; Hait, D.; Hoffmann, M. R.; Lee, S.; Levine, D. S.; Magoulas, I.; Shen, J., et al. The ground state electronic energy of benzene. *The Journal of Physical Chemistry Letters* **2020**, *11*, 8922–8929.

¹⁰²Dunning Jr, T. H. Gaussian basis sets for use in correlated molecular calculations. I. The atoms boron through neon and hydrogen. *The Journal of Chemical Physics* **1989**, *90*, 1007–1023.

¹⁰³Ronca, E.; Li, Z.; Jimenez-Hoyos, C. A.; Chan, G. K.-L. Time-step targeting time-dependent and dynamical density matrix renormalization group algorithms with ab initio Hamiltonians. *Journal of Chemical Theory and Computation* **2017**, *13*, 5560–5571.

¹⁰⁴Guo, S.; Li, Z.; Chan, G. K.-L. Communication: An efficient stochastic algorithm for the perturbative density matrix renormalization group in large active spaces. *The Journal of Chemical Physics* **2018**, *148*, 221104.

¹⁰⁵White, S. R.; Martin, R. L. Ab initio quantum chemistry using the density matrix renormalization group. *The Journal of Chemical Physics* **1999**, *110*, 4127–4130.

¹⁰⁶Jeckelmann, E.; White, S. R. Density-matrix renormalization-group study of the polaron problem in the Holstein model. *Physical Review B* **1998**, *57*, 6376.

¹⁰⁷Ge, Y.; Li, W.; Ren, J.; Shuai, Z. Computational Method for Evaluating the Thermoelectric Power Factor for Organic Materials Modeled by the Holstein Model: A Time-Dependent Density Matrix Renormalization Group Formalism. *Journal of Chemical Theory and Computation* **2022**, *18*, 6437–6446.

¹⁰⁸Hübiger, C.; McCulloch, I.; Schollwöck, U. Generic construction of efficient matrix product operators. *Physical Review B* **2017**, *95*, 035129.

¹⁰⁹Ren, J.; Li, W.; Jiang, T.; Shuai, Z. A general automatic method for optimal construction of matrix product operators using bipartite graph theory. *The Journal of Chemical Physics* **2020**, *153*, 084118.

¹¹⁰Stoudenmire, E. M.; White, S. R. Sliced basis density matrix renormalization group for electronic structure. *Physical Review Letters* **2017**, *119*, 046401.

¹¹¹Lin, L.; Tong, Y. Low-rank representation of tensor network operators with long-range pairwise interactions. *SIAM Journal on Scientific Computing* **2021**, *43*, A164–A192.

¹¹²Kirn, J.; Rees, D. Crystallographic structure and functional implications of the nitrogenase molybdenum–iron protein from *Azotobacter vinelandii*. *Nature* **1992**, *360*, 553–560.

¹¹³Sharma, S.; Chan, G. K.-L. Communication: A flexible multi-reference perturbation theory by minimizing the Hylleraas functional with matrix product states. *The Journal of Chemical Physics* **2014**, *141*, 111101.

¹¹⁴Shewchuk, J. R., et al. An introduction to the conjugate gradient method without the agonizing pain. 1994.

¹¹⁵Harman, H. H.; Jones, W. H. Factor analysis by minimizing residuals (minres). *Psychometrika* **1966**, *31*, 351–368.

¹¹⁶Hicken, J. E.; Zingg, D. W. A simplified and flexible variant of GCROT for solving nonsymmetric linear systems. *SIAM Journal on Scientific Computing* **2010**, *32*, 1672–1694.

¹¹⁷Van Gijzen, M. B.; Sonneveld, P. Algorithm 913: An elegant IDR (s) variant that efficiently exploits biorthogonality properties. *ACM Transactions on Mathematical Software* **2011**, *38*, 1–19.

¹¹⁸Mohr, S.; Dawson, W.; Wagner, M.; Caliste, D.; Nakajima, T.; Genovese, L. Efficient computation of sparse matrix functions for large-scale electronic structure calculations: The CheSS library. *Journal of Chemical Theory and Computation* **2017**, *13*, 4684–4698.

¹¹⁹Paige, C. C.; Saunders, M. A. LSQR: An algorithm for sparse linear equations and sparse least squares. *ACM Transactions on Mathematical Software* **1982**, *8*, 43–71.

¹²⁰Zhai, H.; Gao, Y.; Chan, G. K.-L. pyblock3: an efficient python block-sparse tensor and MPS/DMRG library. 2021; <https://github.com/block-hczhai/pyblock3-preview>.

¹²¹Harris, C. R.; Millman, K. J.; Van Der Walt, S. J.; Gommers, R.; Virtanen, P.; Cournapeau, D.; Wieser, E.; Taylor, J.; Berg, S.; Smith, N. J., et al. Array programming with NumPy. *Nature* **2020**, *585*, 357–362.

¹²²Paszke, A.; Gross, S.; Chintala, S.; Chanan, G.; Yang, E.; DeVito, Z.; Lin, Z.; Desmaison, A.; Antiga, L.; Lerer, A. Automatic differentiation in pytorch. **2017**,

¹²³Hirata, S. Tensor contraction engine: Abstraction and automated parallel implementation of configuration-interaction, coupled-cluster, and many-body perturbation theories. *The Journal of Physical Chemistry A* **2003**, *107*, 9887–9897.

¹²⁴Hirata, S. Symbolic algebra in quantum chemistry. *Theoretical Chemistry Accounts* **2006**, *116*, 2–17.

¹²⁵Neuscamman, E.; Yanai, T.; Chan, G. K.-L. Quadratic canonical transformation theory and higher order density matrices. *The Journal of chemical physics* **2009**, *130*, 124102.

¹²⁶Saitow, M.; Kurashige, Y.; Yanai, T. Multireference configuration interaction theory using cumulant reconstruction with internal contraction of density matrix renormalization group wave function. *The Journal of Chemical Physics* **2013**, *139*, 044118.

¹²⁷MacLeod, M. K.; Shiozaki, T. Communication: Automatic code generation enables nuclear gradient computations for fully internally contracted multireference theory. *The Journal of Chemical Physics* **2015**, *142*, 051103.

¹²⁸Saitow, M.; Kurashige, Y.; Yanai, T. Fully internally contracted multireference configuration interaction theory using density matrix renormalization group: A reduced-scaling implementation derived by computer-aided tensor factorization. *Journal of Chemical Theory and Computation* **2015**, *11*, 5120–5131.

¹²⁹Evangelista, F. A. Automatic derivation of many-body theories based on general Fermi vacua. *The Journal of Chemical Physics* **2022**, *157*, 064111.

¹³⁰Saez, T. Relativistic Hamiltonians for chemistry: A primer. *ChemPhysChem* **2011**, *12*, 3077–3094.

¹³¹Schurkus, H.; Chen, D.-T.; Cheng, H.-P.; Chan, G.; Stanton, J. Theoretical prediction of magnetic exchange coupling constants from broken-symmetry coupled cluster calculations. *The Journal of Chemical Physics* **2020**, *152*, 234115.

¹³²Zgid, D.; Nooijen, M. Obtaining the two-body density matrix in the density matrix renormalization group method. *The Journal of Chemical Physics* **2008**, *128*, 144115.

¹³³Guo, S.; Watson, M. A.; Hu, W.; Sun, Q.; Chan, G. K.-L. N-electron valence state perturbation theory based on a density matrix renormalization group reference function, with applications to the chromium dimer and a trimer model of poly (p-phenylenevinylene). *Journal of Chemical Theory and Computation* **2016**, *12*, 1583–1591.

¹³⁴Angeli, C.; Cimiraglia, R.; Malrieu, J.-P. n-electron valence state perturbation theory: A spinless formulation and an efficient implementation of the strongly contracted and of the partially contracted variants. *The Journal of Chemical Physics* **2002**, *117*, 9138–9153.

¹³⁵Legeza, Ö.; Sólyom, J. Optimizing the density-matrix renormalization group method using quantum information entropy. *Physical Review B* **2003**, *68*, 195116.

¹³⁶Boguslawski, K.; Tecmer, P.; Legeza, O.; Reiher, M. Entanglement measures for single-and multireference correlation effects. *The Journal of Physical Chemistry Letters* **2012**, *3*, 3129–3135.

¹³⁷Liu, G.; Li, W.; You, W. Bipartite entanglement of the one-dimensional extended quantum compass model in a transverse field. *The European Physical Journal B* **2012**, *85*, 1–6.

¹³⁸Lee, S.; Zhai, H.; Sharma, S.; Umrigar, C. J.; Chan, G. K.-L. Externally corrected ccSD with renormalized perturbative triples (R-ecCCSD (T)) and the density matrix renormalization group and selected configuration interaction external sources. *Journal of Chemical Theory and Computation* **2021**, *17*, 3414–3425.

¹³⁹Magoulas, I.; Gururangan, K.; Piecuch, P.; Deustua, J. E.; Shen, J. Is externally corrected coupled cluster always better than the underlying truncated configuration interaction? *Journal of Chemical Theory and Computation* **2021**, *17*, 4006–4027.

¹⁴⁰Kinoshita, T.; Hino, O.; Bartlett, R. J. Coupled-cluster method tailored by configuration interaction. *The Journal of Chemical Physics* **2005**, *123*.

¹⁴¹Hino, O.; Kinoshita, T.; Chan, G. K.-L.; Bartlett, R. Tailored coupled cluster singles and doubles method applied to calculations on molecular structure and harmonic vibrational frequencies of ozone. *The Journal of Chemical Physics* **2006**, *124*, 114311–114311.

¹⁴²Veis, L.; Antalík, A.; Brabec, J.; Neese, F.; Legeza, O.; Pittner, J. Coupled cluster method with single and double excitations tailored by matrix product state wave functions. *The Journal of Physical Chemistry Letters* **2016**, *7*, 4072–4078.

¹⁴³Faulstich, F. M.; Máté, M.; Laestadius, A.; Csirik, M. A.; Veis, L.; Antalík, A.; Brabec, J.; Schneider, R.; Pittner, J.; Kvaal, S., et al. Numerical and theoretical aspects of the DMRG-TCC method exemplified by the nitrogen dimer. *Journal of Chemical Theory and Computation* **2019**, *15*, 2206–2220.

¹⁴⁴Mitrushchenkov, A. O.; Fano, G.; Linguerri, R.; Palmieri, P. On the importance of orbital localization in QC-DMRG calculations. *International Journal of Quantum Chemistry* **2012**, *112*, 1606–1619.

¹⁴⁵Shepard, R.; Brozell, S. R.; Gidofalvi, G. The representation and parametrization of orthogonal matrices. *The Journal of Physical Chemistry A* **2015**, *119*, 7924–7939.

¹⁴⁶Kuhn, H. W. The Hungarian method for the assignment problem. *Naval Research Logistics Quarterly* **1955**, *2*, 83–97.

¹⁴⁷Fukuda, K.; Matsui, T. Finding all the perfect matchings in bipartite graphs. *Applied Mathematics Letters* **1994**, *7*, 15–18.

¹⁴⁸Ramasesha, S.; Pati, S. K.; Krishnamurthy, H.; Shuai, Z.; Brédas, J. Low-lying electronic excitations and nonlinear optical properties of polymers via symmetrized density matrix renor-

malization group method. *Synthetic Metals* **1997**, *85*, 1019–1022.

¹⁴⁹Dorando, J. J.; Hachmann, J.; Chan, G. K.-L. Analytic response theory for the density matrix renormalization group. *The Journal of Chemical Physics* **2009**, *130*, 184111.

¹⁵⁰Lee, S.; Zhai, H.; Chan, G. K.-L. An ab initio correction vector restricted active space approach to the L-edge XAS and 2p3d RIXS spectra of transition metal clusters. *arXiv preprint arXiv:2305.08184* **2023**.

¹⁵¹Wathen, A. J. Preconditioning. *Acta Numerica* **2015**, *24*, 329–376.

¹⁵²Holzner, A.; Weichselbaum, A.; McCulloch, I. P.; Schollwöck, U.; von Delft, J. Chebyshev matrix product state approach for spectral functions. *Physical Review B* **2011**, *83*, 195115.

¹⁵³Braun, A.; Schmitteckert, P. Numerical evaluation of Green's functions based on the Chebyshev expansion. *Physical Review B* **2014**, *90*, 165112.

¹⁵⁴Xie, H.; Huang, R.; Han, X.; Yan, X.; Zhao, H.; Xie, Z.; Liao, H.; Xiang, T. Reorthonormalization of Chebyshev matrix product states for dynamical correlation functions. *Physical Review B* **2018**, *97*, 075111.

¹⁵⁵Jiang, T.; Ren, J.; Shuai, Z. Chebyshev matrix product states with canonical orthogonalization for spectral functions of many-body systems. *The Journal of Physical Chemistry Letters* **2021**, *12*, 9344–9352.

¹⁵⁶Haegeman, J.; Cirac, J. I.; Osborne, T. J.; Pižorn, I.; Verschelde, H.; Verstraete, F. Time-dependent variational principle for quantum lattices. *Physical Review Letters* **2011**, *107*, 070601.

¹⁵⁷Kinder, J. M.; Ralph, C. C.; Chan, G. K.-L. Analytic Time Evolution, Random Phase Approximation, and Green Functions for Matrix Product States. *arXiv preprint arXiv:1103.2155* **2011**.

¹⁵⁸Nakatani, N.; Wouters, S.; Van Neck, D.; Chan, G. K.-L. Linear response theory for the density matrix renormalization group: Efficient algorithms for strongly correlated excited states. *The Journal of Chemical Physics* **2014**, *140*, 024108.

¹⁵⁹Haegeman, J.; Lubich, C.; Oseledets, I.; Vandereycken, B.; Verstraete, F. Unifying time evolution and optimization with matrix product states. *Physical Review B* **2016**, *94*, 165116.

¹⁶⁰Heidrich-Meisner, F.; Feiguin, A. E.; Dagotto, E. Real-time simulations of nonequilibrium transport in the single-impurity Anderson model. *Physical Review B* **2009**, *79*, 235336.

¹⁶¹Jiang, T.; Li, W.; Ren, J.; Shuai, Z. Finite temperature dynamical density matrix renormalization group for spectroscopy in frequency domain. *The Journal of Physical Chemistry Letters* **2020**, *11*, 3761–3768.

¹⁶²Ren, J.; Shuai, Z.; Chan, G. K.-L. Time-dependent density matrix renormalization group algorithms for nearly exact absorption and fluorescence spectra of molecular aggregates at both zero and finite temperature. *Journal of Chemical Theory and Computation* **2018**, *14*, 5027–5039.

¹⁶³Peng, R.; White, A. F.; Zhai, H.; Kin-Lic Chan, G. Conservation laws in coupled cluster dynamics at finite temperature. *The Journal of Chemical Physics* **2021**, *155*, 044103.

¹⁶⁴Loos, P.-F.; Gill, P. M. The uniform electron gas. *Wiley Interdisciplinary Reviews: Computational Molecular Science* **2016**, *6*, 410–429.

¹⁶⁵Szalay, P. G.; Muller, T.; Gidofalvi, G.; Lischka, H.; Shepard, R. Multiconfiguration self-consistent field and multireference configuration interaction methods and applications. *Chemical Reviews* **2012**, *112*, 108–181.

¹⁶⁶Yanai, T.; Kurashige, Y.; Neuscamman, E.; Chan, G. K.-L. Multireference quantum chemistry through a joint density matrix renormalization group and canonical transformation theory. *The Journal of chemical physics* **2010**, *132*, 024105.

¹⁶⁷Kurashige, Y.; Yanai, T. Second-order perturbation theory with a density matrix renormalization group self-consistent field reference function: Theory and application to the study of chromium dimer. *The Journal of Chemical Physics* **2011**, *135*, 094104.

¹⁶⁸Sharma, S.; Alavi, A. Multireference linearized coupled cluster theory for strongly correlated systems using matrix product states. *The Journal of Chemical Physics* **2015**, *143*, 102815.

¹⁶⁹Luo, Z.; Ma, Y.; Wang, X.; Ma, H. Externally-contracted multireference configuration interaction method using a DMRG reference wave function. *Journal of Chemical Theory and Computation* **2018**, *14*, 4747–4755.

¹⁷⁰Sharma, P.; Bernales, V.; Knecht, S.; Truhlar, D. G.; Gagliardi, L. Density matrix renormalization group pair-density functional theory (DMRG-PDFT): singlet–triplet gaps in polyacenes and polyacetylenes. *Chemical Science* **2019**, *10*, 1716–1723.

¹⁷¹Khokhlov, D.; Belov, A. Toward an accurate Ab initio description of low-lying singlet excited states of polyenes. *Journal of Chemical Theory and Computation* **2021**, *17*, 4301–4315.

¹⁷²Guo, S.; Li, Z.; Chan, G. K.-L. A perturbative density matrix renormalization group algorithm for large active spaces. *Journal of Chemical Theory and Computation* **2018**, *14*, 4063–4071.

¹⁷³Sharma, S.; Jeanmairet, G.; Alavi, A. Quasi-degenerate perturbation theory using matrix product states. *The Journal of Chemical Physics* **2016**, *144*, 034103.

¹⁷⁴Sharma, S.; Knizia, G.; Guo, S.; Alavi, A. Combining internally contracted states and matrix product states to perform multireference perturbation theory. *Journal of Chemical Theory and Computation* **2017**, *13*, 488–498.

¹⁷⁵Barcza, G.; Werner, M. A.; Zaránd, G.; Pershin, A.; Benedek, Z.; Legeza, O.; Szilvási, T. Toward Large-Scale Restricted Active Space Calculations Inspired by the Schmidt Decomposition. *The Journal of Physical Chemistry A* **2022**, *126*, 9709–9718.

¹⁷⁶Szalay, P. G.; Bartlett, R. J. Multi-reference averaged quadratic coupled-cluster method: a size-extensive modification of multi-reference CI. *Chemical Physics Letters* **1993**, *214*, 481–488.

¹⁷⁷Gdanitz, R. J.; Ahlrichs, R. The averaged coupled-pair functional (ACPF): A size-extensive modification of MRCI(SD). *Chemical Physics Letters* **1988**, *143*, 413–420.

¹⁷⁸Angeli, C.; Cimiraglia, R.; Evangelisti, S.; Leininger, T.; Malleau, J.-P. Introduction of n-electron valence states for multireference perturbation theory. *The Journal of Chemical Physics* **2001**, *114*, 10252–10264.

¹⁷⁹Angeli, C.; Pastore, M.; Cimiraglia, R. New perspectives in multireference perturbation theory: the n-electron valence state approach. *Theoretical Chemistry Accounts* **2007**, *117*, 743–754.

¹⁸⁰Fink, R. F. Two new unitary-invariant and size-consistent perturbation theoretical approaches to the electron correlation energy. *Chemical Physics Letters* **2006**, *428*, 461–466.

¹⁸¹Fink, R. F. The multi-reference retaining the excitation degree perturbation theory: A size-consistent, unitary invariant, and rapidly convergent wavefunction based ab initio approach. *Chemical Physics* **2009**, *356*, 39–46.

¹⁸²Roemelt, M.; Guo, S.; Chan, G. K. A projected approximation to strongly contracted N-electron valence perturbation theory for DMRG wavefunctions. *The Journal of Chemical Physics* **2016**, *144*, 204113.

¹⁸³Jakob, W.; Rhineland, J.; Moldovan, D. pybind11—Seamless operability between C++11 and Python. 2017; <https://github.com/pybind/pybind11>.

¹⁸⁴Cui, Z.-H.; Zhu, T.; Chan, G. K.-L. Efficient implementation of ab initio quantum embedding in periodic systems: Density matrix embedding theory. *Journal of Chemical Theory and Computation* **2019**, *16*, 119–129.

¹⁸⁵Sun, C.; Ray, U.; Cui, Z.-H.; Stoudenmire, M.; Ferrero, M.; Chan, G. K.-L. Finite-temperature density matrix embedding theory. *Physical Review B* **2020**, *101*, 075131.

¹⁸⁶Cui, Z.-H.; Zhai, H.; Zhang, X.; Chan, G. K.-L. Systematic electronic structure in the cuprate parent state from quantum many-body simulations. *Science* **2022**, *377*, 1192–1198.

¹⁸⁷Cui, Z.-H.; Yang, J.; Tölle, J.; Ye, H.-Z.; Zhai, H.; Kim, R.; Zhang, X.; Lin, L.; Berkelbach, T. C.; Chan, G. K.-L. Ab initio

quantum many-body description of superconducting trends in the cuprates. *arXiv preprint arXiv:2306.16561* **2023**,

¹⁸⁸Zhu, T.; Cui, Z.-H.; Chan, G. K.-L. Efficient formulation of ab initio quantum embedding in periodic systems: Dynamical mean-field theory. *Journal of Chemical Theory and Computation* **2019**, *16*, 141–153.

¹⁸⁹Zhu, T.; Chan, G. K.-L. Ab Initio Full Cell G W+ DMFT for Correlated Materials. *Physical Review X* **2021**, *11*, 021006.

¹⁹⁰Aquilante, F.; Autschbach, J.; Bardi, A.; Battaglia, S.; Borin, V. A.; Chibotaru, L. F.; Conti, I.; De Vico, L.; Delcey, M.; Ferré, N., et al. Modern quantum chemistry with [Open] Molcas. *The Journal of Chemical Physics* **2020**, *152*.

¹⁹¹Liu, F.; Kurashige, Y.; Yanai, T.; Morokuma, K. Multireference ab initio density matrix renormalization group (DMRG)-CASSCF and DMRG-CASPT2 study on the photochromic ring opening of spiropyran. *Journal of Chemical Theory and Computation* **2013**, *9*, 4462–4469.

¹⁹²Wouters, S.; Van Speybroeck, V.; Van Neck, D. DMRG-CASPT2 study of the longitudinal static second hyperpolarizability of all-trans polyenes. *The Journal of Chemical Physics* **2016**, *145*, 054120.

¹⁹³Nakatani, N.; Guo, S. Density matrix renormalization group (DMRG) method as a common tool for large active-space CASSCF/CASPT2 calculations. *The Journal of Chemical Physics* **2017**, *146*, 094102.

¹⁹⁴Kurashige, Y.; Chalupský, J.; Lan, T. N.; Yanai, T. Complete active space second-order perturbation theory with cumulant approximation for extended active-space wavefunction from density matrix renormalization group. *The Journal of Chemical Physics* **2014**, *141*, 174111.

¹⁹⁵Phung, Q. M.; Wouters, S.; Pierloot, K. Cumulant approximated second-order perturbation theory based on the density matrix renormalization group for transition metal complexes: A benchmark study. *Journal of Chemical Theory and Computation* **2016**, *12*, 4352–4361.

¹⁹⁶Li, C.; Evangelista, F. A. Multireference theories of electron correlation based on the driven similarity renormalization group. *Annual Review of Physical Chemistry* **2019**, *70*, 245–273.

¹⁹⁷Qiskit contributors, Qiskit: An Open-source Framework for Quantum Computing. 2023; <https://github.com/Qiskit/qiskit>.